

# Distribution-Free Calibration of Statistical Confidence Sets

**Luben M. C. Cabezas**

LUCRUZ45.CAB@GMAIL.COM

*Department of Statistics and Institute of Mathematics and Computer Science  
Federal University of São Carlos and University of São Paulo  
São Carlos, SP 13565-905 and 13566-590, Brazil*

**Guilherme P. Soares**

GUI.PEDRI.SOARES@GMAIL.COM

*Institute of Mathematics and Computer Science  
University of São Paulo  
São Carlos, SP 13566-590, Brazil*

**Thiago R. Ramos**

THIAGORR@UFSCAR.BR

*Department of Statistics  
Federal University of São Carlos  
São Carlos, SP 13565-905, Brazil*

**Rafael B. Stern**

RBSTERN@GMAIL.COM

*Institute of Mathematics and Statistics  
University of São Paulo  
São Paulo, SP 05508-090, Brazil*

**Rafael Izbicki**

RAFAELIZBICKI@GMAIL.COM

*Department of Statistics  
Federal University of São Carlos  
São Carlos, SP 13565-905, Brazil*

## Abstract

Constructing valid confidence sets is a crucial task in statistical inference, yet traditional methods often face challenges when dealing with complex models or limited observed sample sizes. These challenges are frequently encountered in modern applications, such as Likelihood-Free Inference (LFI). In these settings, confidence sets may fail to maintain a confidence level close to the nominal value. In this paper, we introduce two novel methods, **TRUST** and **TRUST++**, for calibrating confidence sets to achieve distribution-free conditional coverage. These methods rely entirely on simulated data from the statistical model to perform calibration. Leveraging insights from conformal prediction techniques adapted to the statistical inference context, our methods ensure both finite-sample local coverage and asymptotic conditional coverage as the number of simulations increases, even if  $n$  is small. They effectively handle nuisance parameters and provide computationally efficient uncertainty quantification for the estimated confidence sets. This allows users to assess whether additional simulations are necessary for robust inference. Through theoretical analysis and experiments on models with both tractable and intractable likelihoods, we demonstrate that our methods outperform existing approaches, particularly in small-sample regimes. This work bridges the gap between conformal prediction and statistical inference, offering practical tools for constructing valid confidence sets in complex models.

**Keywords:** confidence sets, distribution-free inference, likelihood-free inference, nuisance parameters, uncertainty quantification, conformal prediction, finite-sample coverage

## 1 Introduction

Confidence sets are fundamental tools in statistical inference, allowing researchers to constrain the value of a parameter  $\theta \in \Theta$  based on observed data  $\mathbf{x} \in \mathcal{X}$ . A confidence set  $R(\mathbf{x}) \subset \Theta$  is considered valid from a frequentist perspective if it satisfies the condition

$$\mathbb{P}(\theta \in R(\mathbf{X})|\theta) = 1 - \alpha \quad \forall \theta \in \Theta, \quad (1)$$

where  $\alpha \in (0, 1)$  is a predefined significance level. This means that  $R$  must achieve the correct coverage regardless of the true value of  $\theta$ .

Traditional methods for constructing confidence sets, such as those detailed in standard textbooks (DeGroot and Schervish, 2012; Schervish, 2012; Casella and Berger, 2024), are often inadequate when applied to complex modern models. For instance, constructing confidence sets for mixture models is notably challenging because standard asymptotic results may not hold (Chen and Li, 2009; Wichitchan et al., 2019). Additionally, many traditional methods rely on asymptotic distributions, making them unsuitable for problems with small sample sizes ( $n$ ).

The challenges become more difficult in Likelihood-Free Inference (LFI) scenarios, where the statistical model is implicitly defined by a complex simulator of  $\mathbf{X}|\theta$  and the likelihood function is intractable (Izbicki et al., 2014; Lueckmann et al., 2019; Izbicki et al., 2019; Papamakarios et al., 2019; Cranmer et al., 2020). In such cases, test statistics must be estimated, and as a result, traditional methods for constructing confidence sets often perform poorly (Dalmasso et al., 2021).

This work aims to calibrate confidence sets to achieve conditional coverage (Equation 1), even for challenging models. We focus on confidence sets defined as:

$$R(\mathbf{X}) := \{\theta \in \Theta \mid \tau(\mathbf{X}, \theta) \geq C_\theta\}, \quad (2)$$

where the cutoff  $C_\theta$  is chosen to ensure conditional coverage, and  $\tau$  measures the plausibility that  $\mathbf{X}$  was generated from  $\theta$  (in the language of hypothesis tests,  $\tau$  is a test statistic). We assume  $\tau$  is fixed (see Sections 1.1.1 and 1.1.2 for details on its selection) and provide tools for calibrating  $C_\theta$ .

Our calibration process only assumes the availability of a simulated dataset of independent pairs,  $\{(\theta_1, \mathbf{X}_1), \dots, (\theta_B, \mathbf{X}_B)\}$ , where each  $\theta_b$  is drawn from some reference distribution  $r(\theta)$  and each  $\mathbf{X}_b$  is generated from the statistical model with parameters  $\theta_b$ , i.e.,  $\mathbf{X}_b \sim \mathbf{X} \mid \theta_b$ . We assume that  $\tau(\mathbf{X}, \theta)|\theta$  is strictly continuous for every  $\theta$ . Note that each  $\mathbf{X}_b$  represents the entire dataset that may be observed, rather than a single sample point.

**Novelty.** While several methods have been proposed to calibrate  $C_\theta$  for general problems (Section 1.1), our method offers several new contributions:

1. **Distribution-free guarantees with  $B$ -asymptotic conditional coverage.** Our approach constructs confidence sets  $\widehat{R}_B(\mathbf{X}) := \{\theta \in \Theta \mid \tau(\mathbf{X}, \theta) \geq \widehat{C}_\theta\}$  with finite-sample local coverage:

$$\mathbb{P}\left(\theta \in \widehat{R}_B(\mathbf{X}) \mid \theta \in A\right) = 1 - \alpha,$$

where  $A$  is a subset of  $\Theta$  chosen so that

$$\mathbb{P}\left(\theta \in \widehat{R}_B(\mathbf{X}) \mid \theta \in A\right) \approx \mathbb{P}\left(\theta \in \widehat{R}_B(\mathbf{X}) \mid \theta\right).$$

Additionally, our method provides  $B$ -asymptotic conditional coverage:

$$\lim_{B \rightarrow \infty} \mathbb{P} \left( \theta \in \widehat{R}_B(\mathbf{X}) | \theta \right) = 1 - \alpha.$$

Thus, our method is robust to poor estimates of  $C_\theta$ , offering distribution-free guarantees while maintaining  $B$ -asymptotic validity. Notably, this coverage is *not* asymptotic with respect to the size of the observed dataset  $\mathbf{x}$ ,  $n$ , as is common with traditional asymptotic approximations. Instead, it relies solely on the number of simulations,  $B$ , which can generally be increased given sufficient computational resources. Furthermore, the set  $A$  is chosen to ensure that local coverage approximates conditional coverage.

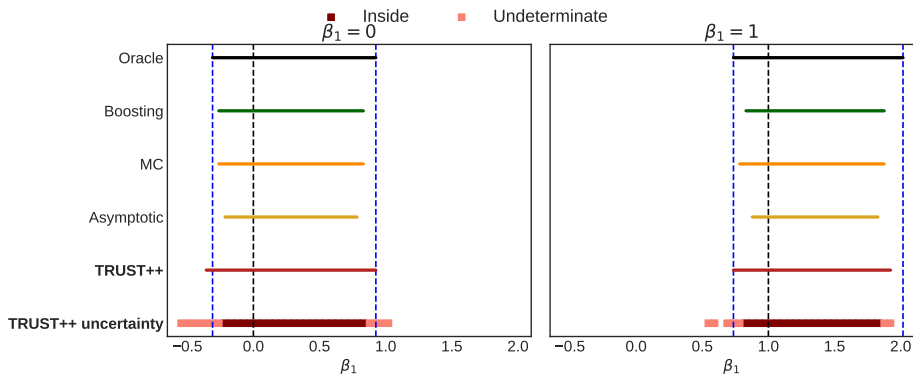
2. **Uncertainty quantification.** In most cases, except for rare instances where  $C_\theta$  can be computed directly (Section 1.1), current methods provide only an estimate  $\widehat{C}_\theta$  of the true  $C_\theta$ . As a result, the confidence intervals produced are only approximations of the true intervals which inherently contain errors. However, these methods do not offer a way to quantify the uncertainty surrounding these estimated intervals. In contrast, our method explicitly constructs confidence sets that provide reliable uncertainty quantification around the estimated confidence intervals. Furthermore, this uncertainty quantification is computationally efficient and does not rely on costly procedures such as bootstrapping. Moreover, it allows users to assess whether additional simulations are necessary for robust inference.
3. **Effective handling of nuisance parameters.** Most models involve nuisance parameters, which are not of direct interest but can complicate inference. Current methods often struggle with properly handling nuisance parameters, particularly when they are numerous, as they typically require expensive numerical maximization algorithms in high-dimensional spaces to ensure coverage (Dalmasso et al., 2021). In contrast, our method significantly reduces the computational burden by transforming the high-dimensional maximization problem into one of finding the maximum over a small, finite set of points, allowing for much more efficient optimization.

Figure 1 compares TRUST++ with other methods for constructing confidence intervals for the slope coefficient in the generalized linear model explored in Section 5.3. Despite the presence of 3 nuisance parameters, TRUST++ produces intervals that are closer to the oracle confidence set, both in terms of size and empirical coverage. It even outperforms traditional GLM confidence sets based on  $\chi^2$  approximations, as well as Monte Carlo-based intervals.

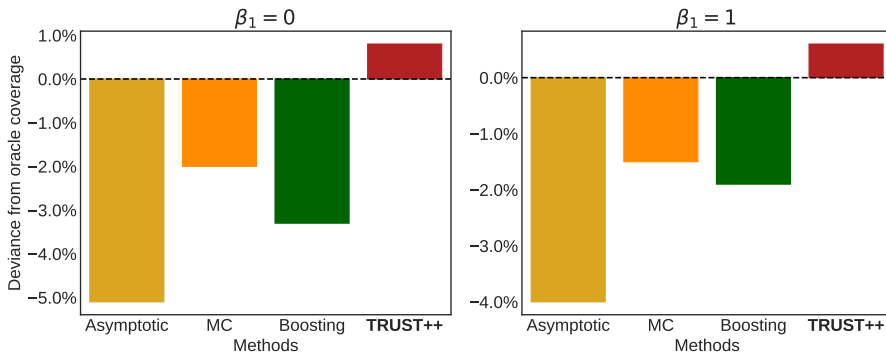
Our tools are developed using insights from conformal prediction techniques (see Section 1.1 for related work). However, while conformal methods focus on generating prediction sets for new labels  $Y$ , which are random variables, statistical inference aims to create confidence sets for a fixed parameter  $\theta$  that generated the data  $\mathbf{x}$ . Thus, conformal techniques need to be adapted to fit this purpose. In particular, asymptotic conditional coverage, which is essential for valid sets, is not guaranteed by standard conformal methods.

We provide two methods:

- TRUST, which uses regression trees to offer a fast approximation to  $C_\theta$ .



(a) 95% confidence intervals. Blue dotted lines represent the lower and upper bounds for the oracle confidence interval.



(b) Deviance from oracle coverage.

Figure 1: Confidence intervals and deviance from oracle coverage comparisons for the GLM example with a sample size of  $n = 50$ . Our method closely approximates the oracle in terms of both the estimated confidence intervals (top) and coverage probabilities (bottom), while also providing uncertainty quantification for the intervals. This feature highlights regions where the true parameter value is more likely to lie. If the undetermined region is large, users can increase the number of simulations to reduce its size and refine the results.

- **TRUST++**, which enhances **TRUST** by employing bagging of trees to deliver more accurate estimates. The extension from trees to forests is non-trivial due to the need for finite sample guarantees.

The remaining of this work is organized as follows: Section 1.1 contains a discussion on related work. Section 2 details the methodology, including the proposed methods and estimation procedures. Section 3 presents the theoretical results. Section 4 discusses implementation details. Section 5 provides applications to examples with tractable likelihood functions, likelihood-free inference, and nuisance parameter problems. Section 6 offers final remarks. Additional materials are provided in Appendices A through C, including experimental details, supplementary algorithms, and complete theoretical proofs.

Finally, all code and supplementary materials are available in the GitHub repository: <https://github.com/Monoxido45/CSI>

## 1.1 Relation to Other Work

### 1.1.1 CLASSICAL CONFIDENCE SETS

Confidence sets typically follow the form described in Equation 2. The function  $\tau(\mathbf{X}, \theta)$  can be a pivotal quantity, which is a quantity whose distribution does not depend on  $\theta$  (e.g.,  $\sigma^{-1}(X - \mu)$  when  $X \sim N(\mu, \sigma)$  and  $\sigma$  is known). Another example of  $\tau(\mathbf{X}, \theta)$  is test statistics used for testing the null hypothesis that the data was generated from  $\theta$ , such as the likelihood ratio statistic  $f(\mathbf{x}|\theta)/\sup_{\theta' \in \Theta} f(\mathbf{x}|\theta')$  (Lehmann et al., 1986).

A key challenge is computing  $C_\theta$ . In simple cases,  $C_\theta$  can be determined in closed form. For instance, when  $\tau$  is a pivotal quantity,  $C_\theta$  does not depend on  $\theta$  and is typically straightforward to find (Casella and Berger, 2024). More often, asymptotic derivations are employed, which are effective only for large sample sizes  $n$  and for certain test statistics (Van der Vaart, 2000). However, these approximations require regularity conditions that frequently fail (Algeri et al., 2019). Similarly, bootstrap methods can be used, but these are effective only for large sample sizes  $n$  and also require regularity conditions (Van der Vaart, 2000).

Our methods instead provide consistent (as  $B$  increases) estimates of  $C_\theta$  for any fixed  $\tau$ , even for small sample sizes  $n$ . We only require a simulated dataset  $\{(\theta_1, \mathbf{X}_1), \dots, (\theta_B, \mathbf{X}_B)\}$ .

### 1.1.2 LIKELIHOOD-FREE INFERENCE

Likelihood-Free Inference (LFI) problems are problems in which the statistical model lack a tractable analytical distribution for  $\mathbf{X}|\theta$ , but it is still possible to generate simulations from it. For a comprehensive review, see Cranmer et al. (2020). In such situations,  $\tau$  needs to be defined from the simulated set as well. For instance, one may use  $\tau(\mathbf{x}, \theta_0)$  as  $\widehat{\mathbf{V}}^{-1}[\theta|\mathbf{x}](\widehat{\mathbb{E}}[\theta|\mathbf{x}] - \theta_0)^2$ , where the conditional mean and variance are estimated using the simulated dataset (Masserano et al., 2023). For other possibilities, see e.g. Brehmer et al. (2020); Dalmaso et al. (2021).

In LFI, once  $\tau$  has been defined,  $C_\theta$  is often estimated via Monte Carlo simulations for each fixed  $\theta$ , but this approach becomes prohibitively expensive in higher-dimensional spaces. Alternatively, Dalmaso et al. (2020, 2021); Masserano et al. (2023) observed that  $C_\theta$  is the  $1 - \alpha$  conditional quantile of  $\tau(\mathbf{X}, \theta)$  on  $\theta$ , and thus used quantile regressors to estimate  $C_\theta$  using the simulated dataset  $\{(\theta_1, \mathbf{X}_1), \dots, (\theta_B, \mathbf{X}_B)\}$ , where  $\theta_b$  is drawn from a reference distribution  $r(\theta)$  and  $\mathbf{X}_b$  is drawn from the statistical model at  $\theta_b$ . These methods recover  $C_\theta$  as  $B \rightarrow \infty$ , but they do not offer finite-sample guarantees.

There is also a substantial body of work on Bayesian LFI, but these methods do not achieve conditional coverage (Eq. 1) even as  $B \rightarrow \infty$  (Hermans et al., 2021).

### 1.1.3 CONFORMAL PREDICTION

Conformal methods have recently emerged as an approach to using data to obtain valid prediction regions under minimal assumptions (Vovk et al., 2005; Shafer and Vovk, 2008; Angelopoulos et al., 2023). Specifically, given exchangeable labeled data  $\{(\mathbf{X}_1, Y_1), \dots, (\mathbf{X}_m, Y_m)\}$ ,

these methods create prediction regions  $R(\mathbf{x})$  such that

$$\mathbb{P}(Y_{m+1} \in R(\mathbf{X}_{m+1})) \geq 1 - \alpha. \quad (3)$$

The first step in a standard conformal method involves creating a conformity score  $\hat{s} : \mathcal{X} \times \mathcal{Y} \rightarrow \mathbb{R}$ , which measures how well the outputs of a regression model predict new labels  $Y \in \mathcal{Y}$ . In a regression setting, a standard choice for the conformity score is the regression residual, given by  $\hat{s}(\mathbf{x}, y) = |y - \widehat{\mathbb{E}}[Y|\mathbf{x}]|$ . The prediction region then takes the form  $R(\mathbf{x}) = \{y : \hat{s}(\mathbf{x}, y) \leq t\}$ , where  $t$  is chosen to be the  $(1 - \alpha)$ -quantile of the residuals  $\hat{s}(\mathbf{x}, y)$  evaluated on a holdout set not used to train  $\hat{s}$ .

The function  $\tau$  used to construct confidence sets can be interpreted as a conformal score  $\widehat{s}$ , and  $\theta$  can be interpreted as  $Y$ . However, statistical theory is typically employed to design  $\tau$  in a way that yields optimal confidence sets, leveraging the known distribution  $f(\mathbf{x} | \theta)$ . Therefore, standard conformal scores are suboptimal for designing  $\widehat{s}$  for confidence sets. Additionally, most conformal scores only deal with univariate  $Y$ , whereas  $\theta$  is generally multivariate (see however [Dheur et al. \(2024\)](#) for approaches that can be used for multivariate  $Y$ 's).

Another key difference between prediction intervals and confidence sets is that  $\theta$  is not random, whereas  $Y$  is. Thus, marginal coverage (Eq. 3) is insufficient for statistical inference problems; typically, coverage for all fixed  $\theta$ 's, corresponding to conditional coverage (Eq. 1), is also desired. This is because the distribution  $r(\theta)$ , used to sample  $\theta$  on the training set, is often arbitrary; it does not encode any randomness observed in the real world. Unfortunately, it is well-known that conditional coverage can't be achieved without strong assumptions ([Lei and Wasserman, 2014](#)). While many conformal approaches aim to achieve conditional coverage asymptotically, they only control coverage conditional on the features  $\mathbf{x}$ , and not  $y$ . The exception to this are label-conditional conformal prediction methods ([Vovk et al., 2014, 2016](#); [Sadinle et al., 2019](#)), but these apply only to classification problems.

Finally, we note that conformal sets have recently been applied to statistical inference ([Patel et al., 2024](#); [Baragatti et al., 2024](#)). While these methods are highly useful, they are designed for a Bayesian framework, where the focus is on controlling marginal coverage over the prior distribution.

#### 1.1.4 PARTITION-BASED CONFORMAL METHODS

Our approach to asymptotically controlling conditional coverage is closely related to the works of [Vovk et al. \(2005\)](#); [Lei and Wasserman \(2014\)](#); [Boström and Johansson \(2020\)](#); [Izbicki et al. \(2020, 2022\)](#). These methods first partition the feature space and then calibrate  $t$  using the conformal approach described in the previous section for each partition element separately. In particular, TRUST is closely related to LoCart ([Cabezas et al., 2024](#)), which creates a data-driven partition of  $\mathcal{X}$  using regression trees designed to ensure that

$$\mathbb{P}(Y_{n+1} \in R(\mathbf{X}_{n+1}) | \mathbf{X}_{n+1}) \approx 1 - \alpha.$$

However, instead of partitioning the feature space  $\mathcal{X}$ , we partition the parameter space  $\Theta$  to achieve coverage conditions on  $\theta$ .

### 1.1.5 CONFORMAL PREDICTIVE DISTRIBUTIONS

Conformal Predictive Distributions (CPDs) are a recent extension of the conformal prediction framework (Vovk et al., 2019, 2020; Jonkers et al., 2024). These aim to model the entire predictive distribution of  $Y$  in a non-parametric way. If a conformal  $\hat{s}$  is isotonic and balanced (Vovk et al., 2020), the CPD for a new test instance  $\mathbf{X}_{n+1}$  is defined as:

$$Q((\mathbf{X}_{n+1}, y), u) := \frac{1}{n} \sum_{i=1}^n \mathbb{I}(\hat{s}(\mathbf{X}_i, Y_i) \leq \hat{s}(\mathbf{X}_{n+1}, y)) + \frac{u}{n}, \quad (4)$$

for each  $y \in \mathbb{R}$  and where  $u \sim U(0, 1)$  serves as a correction term to ensure the continuity of  $Q((\mathbf{X}_{n+1}, y), u)$ .

In simple terms,  $Q$  provides an estimated probability distribution for the test labels  $y$  based on conformity scores. Specifically, if the data is i.i.d.,  $Q$  is valid, meaning that  $Q((\mathbf{X}_{n+1}, y), u)$  follows a uniform distribution (Vovk et al., 2019), and thus  $Q$  is a valid cumulative distribution function. Leveraging the validity of  $Q$ , we construct  $1 - \alpha$  confidence CP prediction intervals by utilizing the specific  $\alpha/2$  and  $1 - \alpha/2$  percentiles of the CPD (Boström et al., 2021).

In this work, we use Conformal Predictive Distributions to estimate the distribution of the test statistic  $\tau(\mathbf{X}, \theta)$ . This approach provides the desired distribution-free properties when estimating  $C_\theta$ . Additionally, our CPDs allow for the computation of p-values for hypotheses of interest. However, directly using the definition from Eq. 4 for statistical inference problems will not lead to consistent intervals for any fixed  $\theta$ . The percentiles of  $Q$  would not depend on  $\theta$ , which is the same issue discussed in Section 1.1.3. To address this, we employ a local CPD based on a partition of  $\Theta$ . We note that Boström et al. (2021) also constructs CPDs based on partitions, but these partitions are made in  $\mathcal{X}$  rather than in  $\Theta$ . While this approach is valuable for prediction tasks, it does not address the problem of statistical inference.

## 2 Methodology

Fix a test statistic  $\tau$ , and let  $H(\cdot|\theta)$  denote the distribution of  $\tau(\mathbf{X}, \theta)$  given  $\theta$ , that is, for each  $\tau_0 \in \mathbb{R}$ , let

$$H(\tau_0|\theta) := \mathbb{P}(\tau(\mathbf{X}, \theta) \leq \tau_0|\theta).$$

Now, notice that for the confidence set from Equation 2 to have a  $(1 - \alpha)$  confidence level,  $C_\theta$  must satisfy

$$1 - \alpha = \mathbb{P}(\theta \in R(\mathbf{X})|\theta) = \mathbb{P}(\tau(\mathbf{X}, \theta) \geq C_\theta|\theta).$$

In other words, we need  $\mathbb{P}(\tau(\mathbf{X}, \theta) \leq C_\theta) = \alpha$ , which implies that  $C_\theta$  is connected to the CDF  $H$  by

$$C_\theta = H^{-1}(\alpha|\theta),$$

where  $H^{-1}(\cdot|\theta)$  denotes the generalized inverse of  $H(\cdot|\theta)$ , given by

$$H^{-1}(\lambda) = \inf\{t \in \mathbb{R} : H(t|\theta) \geq \lambda\}.$$

This suggests we derive confidence sets by estimating  $H$  and then using the plugin cutoff

$$\widehat{C}_{\theta,B} = \widehat{H}_B^{-1}(\alpha|\theta).$$

The estimated confidence set will then be

$$\widehat{R}_B(\mathbf{X}) := \left\{ \theta \in \Theta \mid \tau(\mathbf{X}, \theta) \geq \widehat{C}_{\theta,B} \right\}.$$

The estimated conditional CDF  $\widehat{H}_B$  can also be used to test statistical hypothesis of the type  $H_0 : \theta = \theta_0$ . Specifically, p-values can be estimated via

$$\widehat{H}_B(\tau(\mathbf{x}_{\text{obs}}, \theta_0) | \theta_0),$$

where  $\mathbf{x}_{\text{obs}}$  represents the observed data<sup>1</sup>.

We build on this by introducing a novel approach to estimate  $H(\cdot|\theta)$ , which ensures robust properties.

## 2.1 Estimating $H(\cdot|\theta)$

Our first estimator of  $H(\cdot|\theta)$ , TRUST (Tree-based Regression for Universal Statistical Testing), is constructed by partitioning  $\Theta$ . First, we show how any partition of  $\Theta$  can be used to form an estimator of  $H$ . Following that, we discuss how to optimally select such a partition.

### 2.1.1 PARTITION-BASED ESTIMATE

Let  $\mathcal{A}$  be any fixed partition of  $\Theta$  and  $\{(\theta_1, \mathbf{X}_1), \dots, (\theta_B, \mathbf{X}_B)\}$  be the simulated dataset from the statistical model. The cumulative distribution function  $H(\cdot|\theta)$  can be estimated using the empirical cumulative distribution of the  $\theta_b$  values from the simulated set that fall into the same partition element as  $\theta$ . Formally, for each  $t \in \mathbb{R}$ , we define

$$\widehat{H}_B(t|\theta, \mathcal{A}) := \frac{1}{|I_{A(\theta)}|} \sum_{b \in I_{A(\theta)}} \mathbb{I}(\tau(\mathbf{X}_b, \theta_b) \leq t), \quad (5)$$

where  $A(\theta)$  represents the element of  $\mathcal{A}$  containing  $\theta$ , and  $I_{A(\theta)} = \{b \in \{1, \dots, B\} : \theta_b \in A(\theta)\}$  is the set of indices for all  $\theta_b$  values that fall into  $A(\theta)$ .

With this partition-based construction of  $\widehat{H}$ , the plugin cutoff  $\widehat{C}_{\theta,B} = \widehat{H}_B^{-1}(\alpha|\theta)$ , used to estimate confidence sets, corresponds to the  $\alpha$ -quantile of the values  $\{\tau(\mathbf{X}_b, \theta_b) : b \in I_{A(\theta)}\}$ . Also,  $\widehat{H}_B$  is essentially a conditional predictive conformal distribution (Section 1.1.5), with the exception that we do not add the uniform distribution used to ensure continuity as it is not needed here. This method therefore aligns with a partition-based conformal approach. However, unlike standard partition-based conformal methods, the partition  $\mathcal{A}$  must be selected to approximate  $H(\alpha|\theta)$  well. The next section discusses how to choose  $\mathcal{A}$  to achieve this goal.

---

1. Indeed, under the null hypothesis,  $\mathbb{P}(H(\tau(\mathbf{X}_{\text{obs}}, \theta_0)) | \theta_0) \leq \alpha | \theta_0) = \mathbb{P}(\tau(\mathbf{X}_{\text{obs}}, \theta_0) \leq H^{-1}(\alpha | \theta_0) | \theta_0) = H(H^{-1}(\alpha)) = \alpha$ , and therefore  $\widehat{H}_B(\tau(\mathbf{x}_{\text{obs}}, \theta_0) | \theta_0)$  will be a valid p-value if  $H$  is consistently estimated as  $B \rightarrow \infty$ .



### 2.1.2 CHOOSING THE PARTITION: TRUST

TRUST uses the estimator in Equation 5 for a specific partition of  $\Theta$ ,  $\mathcal{A}$ . This partition is chosen by a data-driven optimization process designed to yield an accurate estimate of  $H$ . Specifically, TRUST seeks for the coarsest partition such that all  $\theta$ 's that fall into the same element will share a similar conditional distribution  $H(\cdot|\theta)$ . This choice will guarantee that

$$\mathbb{P}\left(\theta \in \widehat{R}_B(\mathbf{X})|\theta\right) \approx \mathbb{P}\left(\theta \in \widehat{R}_B(\mathbf{X})|\theta \in A\right) = 1 - \alpha.$$

In practice, TRUST creates a regression tree that uses  $\theta$  as input and outputs  $\tau(\mathbf{x}, \theta)$  using the simulated data  $(\theta_1, \tau(\mathbf{X}_1, \theta_1)), \dots, (\theta_B, \tau(\mathbf{X}_B, \theta_B))$ , which is derived from the original dataset. This tree effectively partitions  $\Theta$ , and this partition has the desired property above (Meinshausen and Ridgeway, 2006, Theorem 1).

Although our theoretical results assume that the data used to construct the optimal partition is separate from the data used to build the empirical CDF in Equation 5 (refer to Section 3 for details), in practice, we do not perform this data split, as it did not yield any performance gains in our experiments. Algorithm 1 outlines the complete TRUST procedure, and Figure 2 provides a graphical visualization of it.

---

**Algorithm 1:** TRUST algorithm

---

**Data:** Simulated dataset  $(\mathbf{X}_1, \theta_1), \dots, (\mathbf{X}_B, \theta_B)$ ; a grid  $\Theta_{grid} \subseteq \Theta$

**Result:** The confidence set  $\widehat{R}_B(\mathbf{X})$

compute  $\mathcal{I} = (\theta_1, \tau(\mathbf{X}_1, \theta_1)), \dots, (\theta_B, \tau(\mathbf{X}_B, \theta_B))$ ;

split  $\mathcal{I}$  in  $\mathcal{I}_{train}$  and  $\mathcal{I}_{cal}$ , where  $\mathcal{I}_{train} \cap \mathcal{I}_{cal} = \emptyset$ ;

fit a decision tree  $\widehat{g}$  with  $\mathcal{I}_{train}$ :  $\widehat{g}(\theta) \approx \mathbb{E}[\tau(\mathbf{X}, \theta) | \theta]$ ;

$\widehat{g}$  will create a partition  $\widehat{\mathcal{A}}_{train} = \{A_1, \dots, A_K\}$  of  $\Theta$ ;

**for**  $\theta \in \Theta_{grid}$  **do**

$A(\theta) \leftarrow$  element of  $\widehat{\mathcal{A}}_{train}$  where  $\theta$  falls;

$J_{A(\theta)} \leftarrow \{i \in [\mathcal{I}_{cal}] : \theta_i \in A(\theta)\}$ ;

$\widehat{C}_{\theta,B} \leftarrow \alpha$ -quantile of  $\{\tau(\mathbf{X}_c, \theta_c)\}_{c \in J_{A(\theta)}}$ ;

**end**

**return**  $\widehat{R}_B(\mathbf{X}) = \{\theta^* \in \Theta_{grid} \mid \tau(\mathbf{X}, \theta^*) \geq \widehat{C}_{\theta^*,B}\}$

---

## 2.2 From trees to forests: TRUST++

Since a single regression tree often lacks expressiveness, we extend our approach to random forests. However, averaging the  $\widehat{C}_{\theta,B}$  values obtained across trees does not ensure distribution-free guarantees (Cabezas et al., 2024). Instead, we use a random forest to design a new partition of  $\Theta$ , and then apply the methodology described in Section 2.1.1. Specifically, we first create  $K$  TRUST regression trees, each on a different bootstrap sample of the simulated dataset  $\{(\theta_1, \mathbf{X}_1), \dots, (\theta_B, \mathbf{X}_B)\}$ . Next, let  $\rho(\theta', \theta)$  denote Breiman's proximity measure (Breiman, 2001), which counts the number of times  $\theta'$  and  $\theta$  appear in the same leaf across the  $T$  trees. Finally, we define the partition  $\mathcal{A}$  as the partition induced by

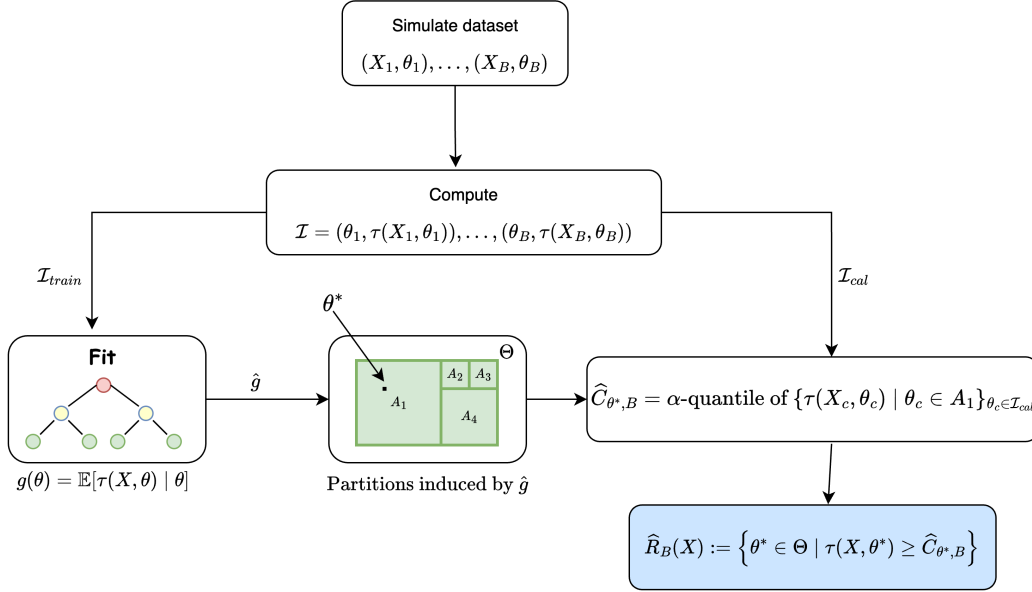


Figure 2: Schematic flowchart of TRUST. Over a simulated dataset  $(\mathbf{X}_1, \theta_1), \dots, (\mathbf{X}_B, \theta_B)$ , we compute the statistic  $\tau$  and create the set  $\mathcal{I}$ , which is splitted between  $\mathcal{I}_{train}$  and  $\mathcal{I}_{cal}$ .  $\mathcal{I}_{train}$  is used to train a regression tree that predicts  $\tau(\mathbf{X}, \theta)$  using  $\theta$ . The tree partitions the parametric space in  $A_1, \dots, A_k$ . If a  $\theta^*$ , from the grid, falls inside the  $A_1$  partition then, in order to calculate the cutoff  $\hat{C}_{\theta^*, B}$ , we will compute the  $\alpha$ -quantile of all  $\tau(\mathbf{X}, \theta)$ 's from which  $\theta$  belongs both to  $\mathcal{I}_{cal}$  and  $A_1$ . Finally, we use the calculated cutoff to find the confidence set  $\hat{R}_B$ .

the equivalence relation

$$\theta \sim \theta' \iff \rho(\theta', \theta) = K.$$

That is, two  $\theta$ 's belong to the same element of  $\mathcal{A}$  if and only if they fall into the same leaves on all trees. Thus, each element  $A \in \mathcal{A}$  consists of parameter values that tend to co-occur in the same leaves across multiple trees in the random forest, and therefore share a similar value of  $H(\cdot|\theta)$ .

We also use a generalized version of TRUST++ that uses

$$A(\theta) := \{\theta' \in \Theta \mid \rho(\theta', \theta) \geq M\},$$

where  $M$  is a tuning parameter in Equation 5.  $M$  can be interpreted as the minimal number of trees required to vote for  $\theta$  and  $\theta'$  to be in the same partition element. See Section 4 for details on how we choose it in practice. Although this version does not always control coverage for  $M < K$  (Guan, 2023), since it does not induce a partition, in practice it has good performance.

TRUST++ can also be framed as a specific instance of the LCP framework by utilizing a box kernel with the Breiman proximity measure replacing the commonly used Euclidean distance. This adaptation allows us to leverage the conformalization procedures from Guan (2023) and Hore and Barber (2023) to transform TRUST++ into a proper conformal method,

thereby ensuring exact coverage control. In this setting, the tuning parameter  $M$  serves as a kernel bandwidth, regulating the granularity of the partition  $\mathcal{A}$ .

Algorithm 2 summarizes the non-conformalized version of our method, which we name TRUST++, and Figure 3 shows the flowchart of the procedure.

---

**Algorithm 2:** TRUST++ algorithm

---

**Data:** Simulated dataset  $(\mathbf{X}_1, \theta_1), \dots, (\mathbf{X}_B, \theta_B)$ ; a grid  $\Theta_{grid} \subseteq \Theta$   
**Result:** The confidence set  $\widehat{R}_B(\mathbf{X})$   
compute  $\mathcal{I} = (\theta_1, \tau(\mathbf{X}_1, \theta_1)), \dots, (\theta_B, \tau(\mathbf{X}_B, \theta_B))$ ;  
split  $\mathcal{I}$  in  $\mathcal{I}_{train}$  and  $\mathcal{I}_{cal}$ , where  $\mathcal{I}_{train} \cap \mathcal{I}_{cal} = \emptyset$ ;  
draw  $K$  bootstrapped samples from  $\mathcal{I}_{train}$ ;  
fit  $K$  TRUST trees, each one with a different sample (Alg. 1);  
**for**  $\theta \in \Theta_{grid}$  **do**  
     $A(\theta) \leftarrow \{\theta' \in \Theta \mid \rho(\theta', \theta) \geq M\}$ , where  $\rho(\theta', \theta)$  is the Breiman's proximity  
    measure and  $M$  a tuning parameter;  
     $J_{A(\theta)} \leftarrow \{i \in [\mathcal{I}_{cal}] : \theta_i \in A(\theta)\}$ ;  
     $\widehat{C}_{\theta, B} \leftarrow \alpha$ -quantile of  $\{\tau(\mathbf{X}_c, \theta_c)\}_{c \in J_{A(\theta)}}$ ;  
**end**  
**return**  $\widehat{R}_B(\mathbf{X}) = \{\theta^* \in \Theta_{grid} \mid \tau(\mathbf{X}, \theta^*) \geq \widehat{C}_{\theta^*, B}\}$

---

### 2.3 Nuisance parameters

Statistical models often have nuisance parameters, which are parameters that are not of direct interest but must be accounted for in the analysis. Suppose that the vector of parameters can be decomposed  $\theta = (\mu, \nu)$ , where  $\mu \in M$  are the parameters of interest and  $\nu \in N$  are nuisance parameters. Our goal is to construct a prediction region for  $\mu$  alone.

Let  $\tau(\mathbf{X}, \mu)$  be a metric that evaluates how plausible it is that  $\mu$  generated  $\mathbf{X}$ . Confidence sets typically have the following form

$$R(\mathbf{x}) := \{\mu : \tau(\mathbf{x}, \mu) \geq C_\mu\}.$$

To control conditional coverage for every  $\mu$  and  $\nu$ , we must set

$$C_\mu = \inf_{\nu} C_{\mu, \nu}, \tag{6}$$

where  $C_{\mu, \nu}$  controls conditional coverage at  $(\mu, \nu)$  (Dalmasso et al., 2021). We now describe how to estimate  $C_\mu$  using our proposed methods.

Let  $H(\cdot | \mu, \nu)$  be the distribution of  $\tau(\mathbf{X}, \mu)$  conditional on  $(\mu, \nu)$ . We use the same methodology, TRUST or TRUST++, to estimate  $H$ , namely by using trees to regress  $\tau(\mathbf{X}, \mu)$  on  $(\mu, \nu)$ . Let  $\widehat{H}_B$  be this estimate. Then, we estimate  $C_\mu$  via

$$\widehat{C}_{\mu, B} = \inf_{\nu} \widehat{H}_B^{-1}(1 - \alpha | \mu, \nu). \tag{7}$$

Although computing the infimum in this equation might seem computationally expensive, the problem is simplified because  $\widehat{H}_B$  is computed using a partition of  $\Theta$ . This means

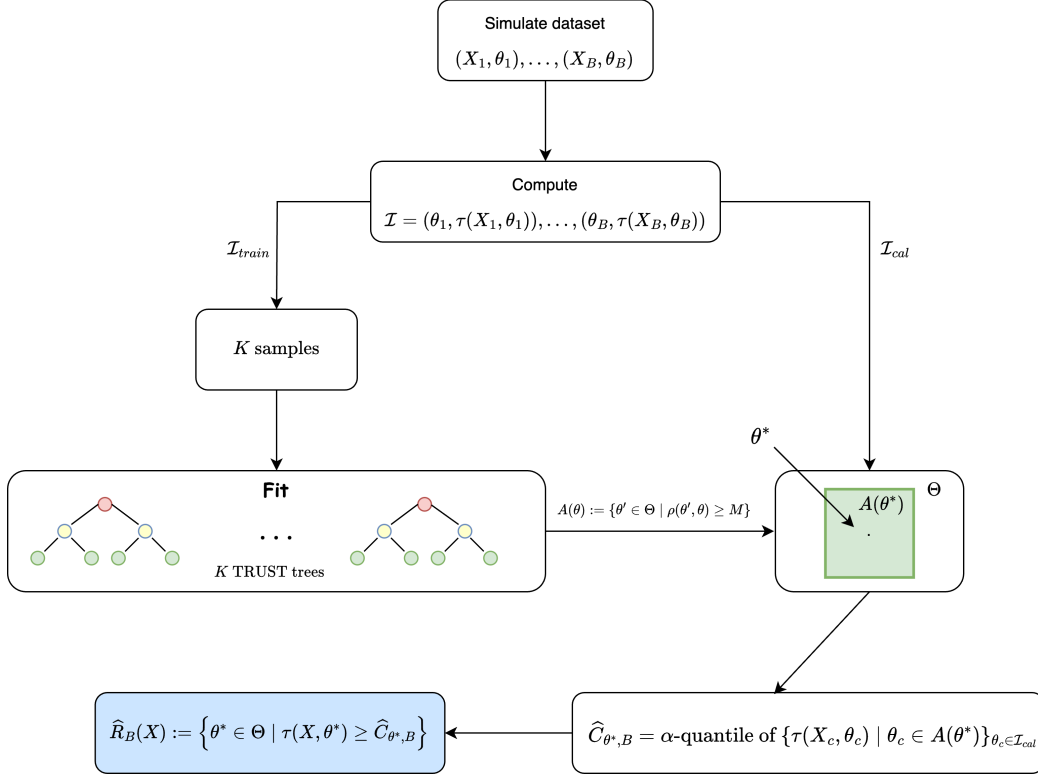


Figure 3: Schematic flowchart of TRUST++. Over a simulated dataset  $(\mathbf{X}_1, \theta_1), \dots, (\mathbf{X}_B, \theta_B)$ , we compute the statistic  $\tau$  and create the set  $\mathcal{I}$ . Then, we draw  $K$  bootstrapped samples over the split  $\mathcal{I}_{train}$  and use each sample to fit a different TRUST tree. The set  $A(\theta)$  is calculated using Breiman’s proximity measure,  $\rho$ , which defines whether two  $\theta, \theta'$  belong to the same partition element. The cutoff  $\widehat{C}_{\theta^*, B}$  is then calculated as the  $\alpha$ -quantile of all  $\tau$  statistics of their respective  $\theta$  that falls over  $A(\theta)$ , for the  $\theta$ ’s that belong to  $\mathcal{I}_{cal}$ . Lastly, the estimated confidence set  $\widehat{R}_B$  can be calculated using  $\widehat{C}_{\theta^*, B}$ .

that the minimization only requires evaluating  $\widehat{H}_B^{-1}(1 - \alpha|\mu, \nu)$  for a finite number of  $\nu$  values, one for each element of the partition that covers  $\mu$ . For example, in the case of TRUST, this approach only requires minimization over the leaves associated with the given  $\mu$ .

In TRUST++, we exploit the fact that only the values of  $\nu$  that appear in the tree splits are relevant when computing the infimum in Equation 7. Specifically, let  $\mathbb{A} \subset \mathcal{N}$  represent the set of nuisance parameter values involved in the splits of the trees generated by TRUST++. Then, for each fixed  $\mu$ , we can express the infimum as

$$\inf_{\nu} \widehat{H}_B^{-1}(1 - \alpha|\mu, \nu) = \min_{\nu \in \mathbb{G}} \widehat{H}_B^{-1}(1 - \alpha|\mu, \nu),$$

where  $\mathbb{G} = \{\nu \pm \epsilon : \nu \in \mathbb{A}\}$ , and  $\epsilon$  is a vector of small numbers that perturbs the nuisance parameter values slightly. This works because, for any value of  $\nu$ , there exists a corresponding  $\nu$  in the grid  $\mathbb{G}$  such that both values fall into the same leaf of the tree. Consequently, it

suffices to compute the minimum over  $\nu \in \mathbb{G}$ . To ensure the  $\epsilon$ -neighborhoods around each  $\nu$  value do not overlap,  $\epsilon$  is chosen as one-third of the minimum coordinate-wise distance between all distinct  $\nu \in \mathbb{A}$ .

To reduce the number of grid values, we may select  $\mathbb{A}$  to include only the most relevant nuisance values—those associated with the splits closer to the root of the trees (Hastie et al., 2009). This approach greatly decreases the computational burden of gridding  $N$ , which other methods require, and consequently limits their applicability to low-dimensional settings with few nuisance parameters.

## 2.4 Uncertainty About the Confidence Sets

Our confidence set  $\widehat{R}_B(\mathbf{X}) := \{\theta \in \Theta \mid \tau(\mathbf{X}, \theta) \geq \widehat{C}_\theta\}$  is an estimate of the oracle set  $R(\mathbf{X}) := \{\theta \in \Theta \mid \tau(\mathbf{X}, \theta) \geq C_\theta\}$ , as is the estimate from the other approaches described in Section 1.1. In this section, we explore another advantage of TRUST and TRUST++: They offer a computationally efficient way to approximate the uncertainty associated with these sets, which we describe in what follows.

Recall that, for each  $\theta$ ,  $C_\theta$  is estimated by computing the  $\alpha$ -quantile of the set  $T_{A(\theta)} = \{\tau(\mathbf{X}_b, \theta_b) : b \in I_{A(\theta)}\}$ , while  $C_\theta$  itself is the  $\alpha$ -quantile of the distribution of  $\tau(\mathbf{X}, \theta) \mid \theta$ . Let  $\tau_{A(\theta)}^{(i)}$  be the  $i$ -th order statistics of  $T_{A(\theta)}$  and define  $Z := |\{\delta \in T_{A(\theta)} : \delta \leq C_\theta\}|$ , where  $Z$  represents the number of statistics in  $T_{A(\theta)}$  that are less than or equal to the cutoff  $C_\theta$ . Note that if the statistics in  $T_{A(\theta)}$  are identically distributed, then  $Z \sim \text{Binomial}(n, 1 - \beta)$ . Using this result, we adapt the method by Hahn and Meeker (2011) for constructing confidence intervals for quantiles to create a  $1 - \beta$  confidence set for  $C_\theta$ . This confidence set is defined as:

$$[\tau_{A(\theta)}^{(l)}, \tau_{A(\theta)}^{(u)}], \tag{8}$$

where  $l$  and  $u$  are selected to satisfy constraints ensuring both the validity and informativeness of the confidence interval. Specifically,  $u$  and  $l$  are selected such that  $l \leq u \leq |I_{A(\theta)}|$  are as close as possible and satisfy the restriction

$$\mathbb{P}(l \leq Z \leq u - 1) \geq 1 - \beta, \tag{9}$$

yielding a valid confidence interval. This is because

$$\mathbb{P}(\tau_{A(\theta)}^{(l)} \leq C_\theta \leq \tau_{A(\theta)}^{(u)}) = \mathbb{P}(l \leq Z \leq u - 1) \geq 1 - \beta.$$

Thus, by choosing  $u$  and  $l$  as narrowly as possible satisfying the restriction from Eq. 9 we get the thinnest valid confidence interval for  $C_\theta$ . Additionally, despite the i.i.d assumption about statistics in  $T_{A(\theta)}$  being not strictly true, the values in  $T_{A(\theta)}$  are approximately identically distributed due to the way the partition was chosen (Section 2.1.2).

For each  $\theta \in \Theta$ , let  $(\widehat{C}_\theta^L, \widehat{C}_\theta^U)$  represent the resulting confidence interval for  $C_\theta$ . The uncertainty can be propagated to the estimated sets by calculating the following three sets:

$$\begin{aligned} \mathcal{I}(\mathbf{X}) &= \{\theta \in \Theta \mid \tau(\mathbf{X}, \theta) \geq \widehat{C}_\theta^U\}, \\ \mathcal{O}(\mathbf{X}) &= \{\theta \in \Theta \mid \tau(\mathbf{X}, \theta) \leq \widehat{C}_\theta^L\}, \text{ and} \\ \mathcal{U}(\mathbf{X}) &= \{\theta \in \Theta \mid \widehat{C}_\theta^L \leq \tau(\mathbf{X}, \theta) \leq \widehat{C}_\theta^U\}, \end{aligned}$$

where  $\mathcal{I}(\mathbf{X})$  represents the set of parameter values confidently inside the confidence interval,  $\mathcal{O}(\mathbf{X})$  contains values confidently outside, and  $\mathcal{U}(\mathbf{X})$  includes those where the status remains uncertain. In the terminology of 3-way hypothesis testing (Berg, 2004; Esteves et al., 2016; Izbicki et al., 2023),  $\mathcal{I}(\mathbf{X})$  is the acceptance region,  $\mathcal{O}(\mathbf{X})$  is the rejection region, and  $\mathcal{U}(\mathbf{X})$  is the agnostic region. The size of  $\mathcal{U}(\mathbf{X})$  can be decreased by increasing the number of simulations used to estimate  $C_\theta$ ,  $B$ . The next theorem shows that this approach controls the probability of incorrect conclusions.

**Theorem 1** Fix  $\mathbf{x} \in \mathcal{X}$  and  $\theta \in \Theta$ . Let  $(\widehat{C}_\theta^L, \widehat{C}_\theta^U)$  represent a  $(1 - \beta)$ -level confidence interval for  $C_\theta$  such that  $\mathbb{P}(C_\theta \leq \widehat{C}_\theta^L) = \mathbb{P}(\widehat{C}_\theta^U \leq C_\theta)$ . Then

$$\mathbb{P}(\theta \in \mathcal{I}(\mathbf{x}) | \theta \notin R(\mathbf{x})) \leq \beta/2$$

and

$$\mathbb{P}(\theta \in \mathcal{O}(\mathbf{x}) | \theta \in R(\mathbf{x})) \leq \beta/2.$$

This method can be readily extended to the setting with nuisance parameters. Let  $\eta^*$  be the configuration of nuisance parameters for which  $\widehat{C}_{\mu, B}$  is computed (Equation 7). By construction,  $\widehat{C}_{\mu, B}$  is the  $\alpha$ -quantile of the set  $T_{A(\mu, \eta^*)} = \{\tau(\mathbf{X}_b, \mu_b, \eta_b) : b \in I_{A(\mu, \eta^*)}\}$ . Thus, we can derive a confidence set for the optimal cutoff using the same approach as in Eq. 8, based now on the set  $T_{A(\mu, \eta^*)}$ .

### 3 Theoretical Results

The key aspect of our method lies in the fact that achieving a good approximation of  $H(\cdot | \theta)$  allows the partitions in TRUST and TRUST++ to effectively capture the local behavior of the test statistic  $\tau$ .

Building on this, our theoretical framework relies on ensuring that  $\widehat{H}_B$  closely approximates  $H$  in both TRUST and TRUST++. This idea is formalized in the following assumption:

**Assumption 1** Let  $\widehat{H}_B$  represent the approximation of  $H$  under either TRUST or TRUST++. For any  $\varepsilon > 0$  and  $\delta > 0$ , there exists a  $B_0 \in \mathbb{N}$  such that, for all  $B \geq B_0$ ,

$$\mathbb{P}\left(\sup_{t \in \mathbb{R}, \theta' \in \Theta} \left| \widehat{H}_B(t | \theta') - H(t | \theta') \right| \leq \varepsilon\right) \geq 1 - \delta.$$

This assumption ensures that, with high probability,  $\widehat{H}_B$  approximates  $H$  as  $B$  increases. This result is supported by theoretical findings, such as those of Meinshausen and Ridgeway (2006); Biau et al. (2008), on the consistency of tree-based models. To guarantee this consistency, certain conditions regarding the distribution of covariates and the structure of the trees are necessary. In tree construction, it is important that node sizes are balanced, with the proportion of observations in each node decreasing as the total number of observations grows. Additionally, each variable must have a minimum probability of being selected for node splitting, and splits should ensure a balanced distribution of observations between subnodes. These assumptions are quite reasonable and enable the conditional distribution estimates to be consistent with the true distribution, providing a solid theoretical foundation for our method.

### 3.1 Partition Coverage Guarantees

As discussed in Section 2.1.1, given any fixed partition  $\mathcal{A}$  of  $\Theta$ , the cumulative distribution function  $H(\cdot|\theta)$  can be estimated empirically using the values of  $\theta_b$  that fall within the same partition element as  $\theta$ . Although a data-agnostic partitioning approach does not guarantee that  $\widehat{H}$  will closely approximate  $H$ , we can still ensure that the plugin cutoff  $\widehat{C}_{\theta,B} = \widehat{H}_B^{-1}(\alpha|\theta)$ , corresponding to the  $\alpha$ -quantile of the values  $\{\tau(\mathbf{X}_b, \theta_b) : b \in I_{A(\theta)}\}$ , achieves the desired coverage when conditioned on the partition element. This result is formalized in the following theorem.

**Theorem 2 (Partition-Based Coverage)** *Let  $\{(\theta_1, \mathbf{X}_1), \dots, (\theta_B, \mathbf{X}_B)\}$  be an i.i.d. simulated dataset with a fixed partition  $\mathcal{A}$  of  $\Theta$ , where each  $\theta_b$  is drawn from a reference distribution  $r(\theta)$  and each  $\mathbf{X}_b$  is generated according to the statistical model with parameters  $\theta_b$ . For a test statistic  $\tau(\mathbf{X}, \theta)$ , consider the confidence set constructed by our method:*

$$\widehat{R}_B(\mathbf{X}) = \{\theta \in \Theta \mid \tau(\mathbf{X}, \theta) \geq \widehat{C}_{\theta,B}\},$$

where  $\widehat{C}_{\theta,B} = \widehat{H}_B^{-1}(\alpha|\theta)$  represents the  $\alpha$ -quantile of the values  $\{\tau(\mathbf{X}_b, \theta_b) : b \in I_{A(\theta)}\}$ , conditioned on  $\theta$  belonging to the partition element  $A(\theta)$ . Then, we have

$$\mathbb{P}(\theta \in \widehat{R}_B(\mathbf{X}) \mid \theta \in A(\theta)) \geq 1 - \alpha,$$

ensuring the desired coverage probability of the confidence set, conditioned on the partition element.

This result applies broadly to any partition, yet it carries particular significance for those formed using TRUST and TRUST++. For these methods, we specifically anticipate the relationship

$$1 - \alpha = \mathbb{P}(\theta \in \widehat{R}_B(\mathbf{X}) \mid \theta \in A(\theta)) \approx \mathbb{P}(\theta \in \widehat{R}_B(\mathbf{X}) \mid \theta),$$

which suggests that, with these methods, the probability that  $\theta$  lies within the estimated region  $\widehat{R}_B(\mathbf{X})$ , given its association with  $A(\theta)$ , closely aligns with the nominal confidence level  $(1 - \alpha)$ . In the following section, we will state the theorem formally and provide additional details surrounding this result.

Beyond the conditional coverage established above, these results also imply marginal coverage, ensuring that the confidence set  $\widehat{R}_B(\mathbf{X})$  maintains the desired overall coverage probability:

**Corollary 1 (Marginal Coverage)** *Let  $\{(\theta_1, \mathbf{X}_1), \dots, (\theta_B, \mathbf{X}_B)\}$  be an i.i.d. simulated dataset with a fixed partition  $\mathcal{A}$  of  $\Theta$ , where each  $\theta_b$  is drawn from a reference distribution  $r(\theta)$  and each  $\mathbf{X}_b$  is generated according to the statistical model with parameters  $\theta_b$ . For a test statistic  $\tau(\mathbf{X}, \theta)$ , consider the confidence set constructed by our method:*

$$\mathbb{P}(\theta \in \widehat{R}_B(\mathbf{X})) \geq 1 - \alpha,$$

ensuring the marginal coverage of the constructed confidence set. In particular, the partition can be taken as that provided by TRUST or TRUST++.

### 3.2 TRUST and TRUST++ Conditional Coverage Guarantees

Both TRUST and TRUST++ employ regression trees that satisfy the consistency Assumption 1, as guaranteed by established results for tree-based models (Meinshausen and Ridgeway, 2006; Biau et al., 2008). With these partitions, we not only guarantee partition-based coverage, as indicated in Theorem 2, but also ensure that both methods asymptotically achieve optimal conditional coverage, as formalized in the next theorem.

**Theorem 3 (*B*-Asymptotic Conditional Coverage)** *Let  $\{(\theta_1, \mathbf{X}_1), \dots, (\theta_B, \mathbf{X}_B)\}$  be an i.i.d. simulated dataset, where each  $\theta_b$  is drawn from a reference distribution  $r(\theta) > 0$  and each  $\mathbf{X}_b$  is generated according to the statistical model with parameters  $\theta_b$ . For a test statistic  $\tau(\mathbf{X}, \theta)$ , consider the confidence set constructed by either TRUST or TRUST++:*

$$\widehat{R}_B(\mathbf{X}) := \{\theta \in \Theta \mid \tau(\mathbf{X}, \theta) \geq \widehat{C}_{\theta, B}\},$$

where  $\widehat{C}_{\theta, B}$  is the cutoff determined by the partition, representing the  $\alpha$ -quantile of the distribution of  $\tau(\mathbf{X}_b, \theta_b)$  values within the partition containing  $\theta$ .

Then, if Assumption 1 holds, both TRUST and TRUST++ are asymptotically consistent, that is:

$$\lim_{B \rightarrow \infty} \mathbb{P}(\theta \in \widehat{R}_B(\mathbf{X}) \mid \theta) = 1 - \alpha.$$

This shows that the partition constructed by TRUST and TRUST++ is designed so that local coverage closely approximates conditional coverage. Moreover, unlike conventional asymptotic approaches, which typically rely on the sample size of the observed dataset  $\mathbf{x}$ ,  $n$ , our approach is independent of  $n$ . Instead, it depends solely on the number of simulations  $B$ , which can be scaled up given sufficient computational resources. This framework enables both TRUST and TRUST++ to achieve robust, distribution-free guarantees and asymptotically attain optimal conditional coverage as  $B$  increases.

In the appendix, we discuss the key results required for the theoretical framework, provide intuition for why our methods work, and present the proofs of the main results.

## 4 Implementation Details and Tuning Parameters

To implement both TRUST and TRUST++, we use the efficient decision tree and random forest implementations provided by *scikit-learn*. Since our approaches use regression trees to partition  $\Theta$ , managing tree growth is crucial to prevent empty or redundant partition elements. This is achieved through both pre and post-pruning. The pre-pruning is executed in both methods by fixing the `min_samples_split` hyperparameter to a value, such as 100 or 300 samples, which enables us to obtain well-populated leaves resulting in more accurate estimations of  $H(\cdot|\theta)$  in our framework.

In TRUST, we additionally apply post-pruning to remove extra leaves and nodes using cost-complexity pruning, balancing partition complexity with predictive performance by reducing the amount of less informative partition elements. Since post-pruning can reduce variability across regression trees and lessen the benefits of ensembling different partitions, it is not applied in TRUST++. For all other hyperparameters of the decision tree and random forest algorithms, we use *scikit-learn*'s default settings, except for the number of trees in the random forest, which we set to 200.



Our default setting for the tuning parameter  $M$  is  $M = K/2$ , placing TRUST++ in a majority-vote regime. In this setup,  $\theta'$  is included in  $A(\theta)$  only if the majority of trees vote for  $\theta'$  and  $\theta$  to be in the same leaf. While this choice is intuitive and performs well in practice (see Section 5.2), it is not universally optimal, as some problems may require larger neighborhoods around  $\theta$  due to the potential approximate non-invariance of statistics.

To address this, we propose a straightforward grid-search algorithm for optimizing  $M$  using a small, additional simulated validation grid. The main idea is to select  $M$  from a fine grid between 0 and  $K$  that minimizes estimated deviation from conditional coverage. This is done by calculating coverage across the validation grid with a batch of statistics simulated at each fixed grid point and then computing the mean absolute error of the estimated coverage relative to the nominal confidence level  $1 - \alpha$ . Section 5 provides further details on this process. Alternatively, coverage can be estimated using the LF2I diagnostic module (Dalmasso et al., 2021), which also leverages an additional simulation set. Algorithm 3 in Appendix B outlines the tuning procedure for  $M$ .

## 5 Applications

In this section, we compare the coverage performance of TRUST and TRUST++ (both tuned and majority-votes versions) to the other state-of-the-art competing methods on tractable likelihood, likelihood-free, and nuisance parameter settings.

To assess performance, we use several statistic and likelihood/simulator combinations across multiple sample sizes  $n$  and simulation budgets  $B$  in both likelihood-based and likelihood-free scenarios. In the nuisance parameter setting, we benchmark our methods with two examples: one using likelihood-free inference and another based on likelihood. We set a common confidence level of  $1 - \alpha = 0.95$  across all experiments. Comparisons are made against the following baseline methods:

- **Gradient Boosting Quantile Regression (Boosting)**: implemented in the *scikit-learn* library (Pedregosa et al., 2011), we use it to estimate  $C_\theta$  through the  $(1 - \alpha)$  conditional quantile of the  $\tau(\mathbf{X}, \theta)$  given  $\theta$  (Dalmasso et al., 2020). We fix the maximum depth as 3, the tolerance for early stopping as 15 and the maximum iteration as 100. The remaining hyperparameters are fixed as *scikit-learn*'s default. To control tree growth in each iteration, we limit the maximum depth to 3 (instead of the default, which is unlimited) and employ a weak learner ensemble approach, which is well-suited for boosting methods (Freund and Schapire, 1997; Hastie et al., 2009).
- **Monte-Carlo (MC)**: implemented with an equally spaced grid over  $\Theta$ , we simulate  $n_{MC}$  statistics for each grid element and estimate  $C_\theta$  using the  $(1 - \alpha)$ -quantile of these simulations at the closest grid point. For multi-dimensional  $\Theta$ , the grid is formed by combining equally spaced one-dimensional grids obtained along each coordinate of  $\Theta$ . To ensure comparability with other methods, the uni-dimensional grid size is set to  $\left\lceil \frac{B}{n_{MC}}^{1/d} \right\rceil$ , where  $d = \dim \Theta$ . This guarantees that the Monte-Carlo simulation budget in multi-dimensional problems will be close to the fixed budget  $B$ . We set in all cases  $n_{MC} = 500$ .

- **Asymptotic:** this approach relies on classic asymptotic results for certain test statistics. It estimates  $C_\theta$  as the  $(1 - \alpha)$ -quantile of the statistic’s asymptotic invariant distribution. Since estimated statistics in the LFI setting lack invariant asymptotic approximations, this method is only applied for comparison in some scenarios with tractable likelihoods.

To evaluate the conditional coverage performance of each approach in both likelihood-based and likelihood-free scenarios, we compute the Mean Absolute Error (MAE) of each method’s conditional coverage concerning the confidence level  $(1 - \alpha)$ . We begin by estimating the conditional coverage of each method through the simulation of several statistics inside an evaluation grid. Let  $\Theta_{\text{grid}}$  denote such a grid. We compute the coverage for each  $\theta' \in \Theta_{\text{grid}}$  at level  $\alpha$  for any cutoff estimation method  $\widehat{C}$  as follows:

$$\text{cover}_\alpha(\widehat{C}, \theta') := \frac{1}{n_{\text{sim}}} \sum_{i=1}^{n_{\text{sim}}} \mathbb{I} \left( \tau(\theta', \mathbf{X}_i^{(\theta')}) \leq \widehat{C}_{\theta'} \right), \quad (10)$$

where  $n_{\text{sim}}$  represents the number of simulated statistics and  $\mathbf{X}_i^{(\theta')}$  denotes the  $i$ -th observation simulated under  $\theta'$ . We then define the MAE of the method’s conditional coverage relative to the nominal confidence level  $(1 - \alpha)$  as:

$$\text{MAE}(\widehat{C}, \alpha) := \frac{1}{|\Theta_{\text{grid}}|} \sum_{\theta' \in \Theta_{\text{grid}}} \left| \text{cover}_\alpha(\widehat{C}, \theta') - (1 - \alpha) \right|. \quad (11)$$

The MAE serves as an effective metric for quantifying the extent to which each method  $\widehat{C}$  deviates from the nominal level of conditional coverage.

In the nuisance scenarios, we assess performance by measuring each method’s coverage deviation from the oracle coverage, defined as follows:

$$d_\alpha(\widehat{C}, C) := \frac{1}{|\Theta_{\text{grid}}|} \sum_{\theta' \in \Theta_{\text{grid}}} \left| \text{cover}_\alpha(\widehat{C}, \theta') - \text{cover}_\alpha(C, \theta') \right|, \quad (12)$$

where  $C$  is the oracle cutoff specified in Eq. 6. This oracle cutoff controls coverage across all parameters—main, and nuisance—by accounting for worst-case variations in the nuisance parameter. Consequently, we compare each method’s coverage against the oracle rather than the nominal level, as the oracle typically over-covers for the parameters of interest to ensure reliable coverage across all nuisance parameters.

We replicate each experiment 50 times for likelihood-based, 30 times for likelihood-free, and 15 times for nuisance examples, and compute the average MAE or deviation from the oracle and its standard error. We identify the top methods in each case as those with the lowest average error, followed by any other methods with performance not significantly different from the best (determined by overlapping 95% asymptotic confidence intervals for the MAE). All computed MAE and standard errors are available in the [supplementary material](#).

### 5.1 Examples with tractable likelihood function

In this section, we apply our methods to construct confidence sets on three standard statistical models. We always assume the data is  $\mathbf{X} = (X_1, \dots, X_n)$ , where the  $X_i$ 's are i.i.d. The models are:

- **Normal model with fixed variance:**  $X_i \stackrel{iid}{\sim} N(\theta, 1)$ , with  $\theta \in \Theta = [-5, 5]$ . When a prior is needed to build  $\tau$ , we use  $\theta \sim N(0, 0.25)$ .
- **Gaussian mixture model (GMM):**  $X_i \stackrel{iid}{\sim} 0.5N(\theta, 1) + 0.5N(-\theta, 1)$ , with  $\theta \in \Theta = [0, 5]$ . When a prior is needed to build  $\tau$ , we use  $\theta \sim N(0.25, 1)$  as the prior.
- **Lognormal model with both mean and scale as parameters:**  $X_i \stackrel{iid}{\sim} \text{lognormal}(\mu, \sigma^2)$ , with  $\boldsymbol{\theta} = \mu \times \sigma^2 \in [-2.5, 2.5] \times [0.15, 1.25] = \Theta$ . When a prior is needed to build  $\tau$ , we use  $(\mu, \sigma^2) \sim \text{NIG}(0, 2, 2, 1)$ .

We explore the following choices of  $\tau$ :

- **Likelihood ratio:** Considering that  $\mathcal{L}(\cdot; \theta_0)$  represents the likelihood function, the likelihood ratio statistic is given by:

$$LR(\mathbf{x}, \theta_0) = \log \frac{\mathcal{L}(\mathbf{x}; \theta_0)}{\sup_{\theta \neq \theta_0} \mathcal{L}(\mathbf{x}; \theta)}. \quad (13)$$

Under regularity conditions, Wilks' theorem (Drton, 2009) implies that  $-2LR(\mathbf{X}, \theta_0)|\theta = \theta_0$  has an asymptotic  $\chi_1^2$  distribution, which is typically used to approximate  $C_\theta$ . However, regularity conditions are not always met, as in the case of the Gaussian Mixture Model (Chen and Li, 2009).

- **Kolmogorov-Smirnov statistic:** Let  $F_{\theta_0}(\cdot)$  be the theoretical CDF under  $\theta_0$  and  $\widehat{F}_n(\cdot)$  be the empirical CDF estimated using data  $\mathbf{X}$  with size  $n$ . The Kolmogorov-Smirnov statistic is defined as:

$$KS(\mathbf{x}, \theta_0) = \sup_{x \in \mathcal{X}} |F_{\theta_0}(x) - \widehat{F}_n(x)| = D_n.$$

In this case, a classical result used to approximate  $C_\theta$  is that, under the null hypothesis:

$$\sqrt{N}D_n \xrightarrow{n \rightarrow \infty} \mathcal{K},$$

with  $\mathcal{K}$  being the Kolmogorov distribution (Marsaglia et al., 2003).

- **Bayes Factor:** Considering a prior probability  $\pi$  over  $\Theta$  and the comparison of the hypothesis  $H_0 : \theta \in \Theta_0$  to its complement  $H_1 : \theta \in \Theta_1$ , the Bayes factor (BF) is given by the ratio of the marginal likelihood of both hypothesis (Kass and Raftery, 1995):

$$BF(\mathbf{x}, \Theta_0) = \frac{\mathbb{P}(\mathbf{x}|H_0)}{\mathbb{P}(\mathbf{x}|H_1)} = \frac{\int_{\Theta_0} \mathcal{L}(\mathbf{x}; \theta) d\pi_0(\theta)}{\int_{\Theta_1} \mathcal{L}(\mathbf{x}; \theta) d\pi_1(\theta)}, \quad (14)$$

where  $\pi_0$  and  $\pi_1$  represent the restrictions of  $\pi$  to  $\Theta_0$  and  $\Theta_1$ , respectively. Since our focus is on the precise hypothesis  $H_0 : \theta = \theta_0$  without altering the joint distribution of the data  $\mathbf{X}$  and  $\theta$ , we define the restrictions as follows:

$$\pi_0(\theta) = \begin{cases} 1 & \text{if } \theta = \theta_0 \\ 0 & \text{otherwise} \end{cases} \quad \pi_1 = \begin{cases} \pi(\theta) & \text{if } \theta \neq \theta_0 \\ 0 & \text{otherwise} \end{cases}$$

and then we compute the Bayes Factor statistic as:

$$BF(\mathbf{x}, \theta_0) = \frac{\int_{\Theta_0} \mathcal{L}(\mathbf{x}; \theta) d\pi_0(\theta)}{\int_{\Theta_1} \mathcal{L}(\mathbf{x}; \theta) d\pi_1(\theta)} = \frac{\mathcal{L}(\mathbf{x}; \theta_0)}{f(\mathbf{x})} = \frac{f(\theta_0, \mathbf{x})}{\pi(\theta_0) \cdot f(\mathbf{x})} = \frac{f(\theta_0|\mathbf{x})}{\pi(\theta_0)}. \quad (15)$$

Following [Dalmasso et al. \(2021\)](#), we use the Bayes Factor as a frequentist statistic to construct confidence sets. We adopt the term ‘‘Bayes Frequentist Statistic’’, as introduced by [Dalmasso et al. \(2021\)](#).

- **E-value:** Another statistic used to test hypotheses in a Bayesian context is the Full Bayesian Significance Testing ([Pereira and Stern, 1999](#); [de B Pereira et al., 2008](#)). This procedure assigns an evidence measure based on the posterior distribution to the hypothesis  $H_0$  and rejects it if the evidence measure is small. Specifically, let  $T_{\theta_0} = \{\theta \in \Theta \mid f(\theta|\mathbf{X}) \geq f(\theta_0|\mathbf{X})\}$ . The Bayesian evidence measure (e-value) in favor of  $H_0$  is defined as:

$$ev(\mathbf{x}, \theta_0) = 1 - \mathbb{P}(\theta \in T_{\theta_0} | \mathbf{x}) = 1 - \int_{T_{\theta_0}} f(\theta|\mathbf{x}) d\theta. \quad (16)$$

Although the e-value is originally considered a Bayesian measure, we use it as a frequentist statistic to construct confidence sets. Therefore, we use the term ‘‘Frequentist e-value’’ to refer to this statistic in our context. [Diniz et al. \(2012\)](#) establishes an asymptotic connection between the e-value and the likelihood ratio statistic, providing an asymptotic approximation for the e-value under contour restrictions. The resulting asymptotic cutoff corresponds to the significance level  $\alpha$  for the simulation settings used here.

To compare all methods, we consider  $n = 1, 10, 50, 100$  and  $B = 1000, 5000, 10000, 15000$  for all combinations of statistic and likelihood, except for the KS statistic, where we start with  $n = 5$  to avoid producing a degenerate estimation of the theoretical CDF  $F_{\theta_0}$ . [Figure 4](#) provides a summary of each method’s performance, while [Figure 5](#) shows the coverage control of each method under varying error bounds, considering only the scenarios where asymptotic cutoffs can be derived. The results highlight several key performance differences among the methods:

- At  $B = 1000$  [Figure 4](#) shows no clear advantage among the methods for different sample sizes  $n$ , with TRUST and tuned TRUST++ showing competitive results in these scenarios. This balance may be attributed to the limited number of simulation samples, which reduces the ability to differentiate among methods regarding cutoff estimation and overall performance.

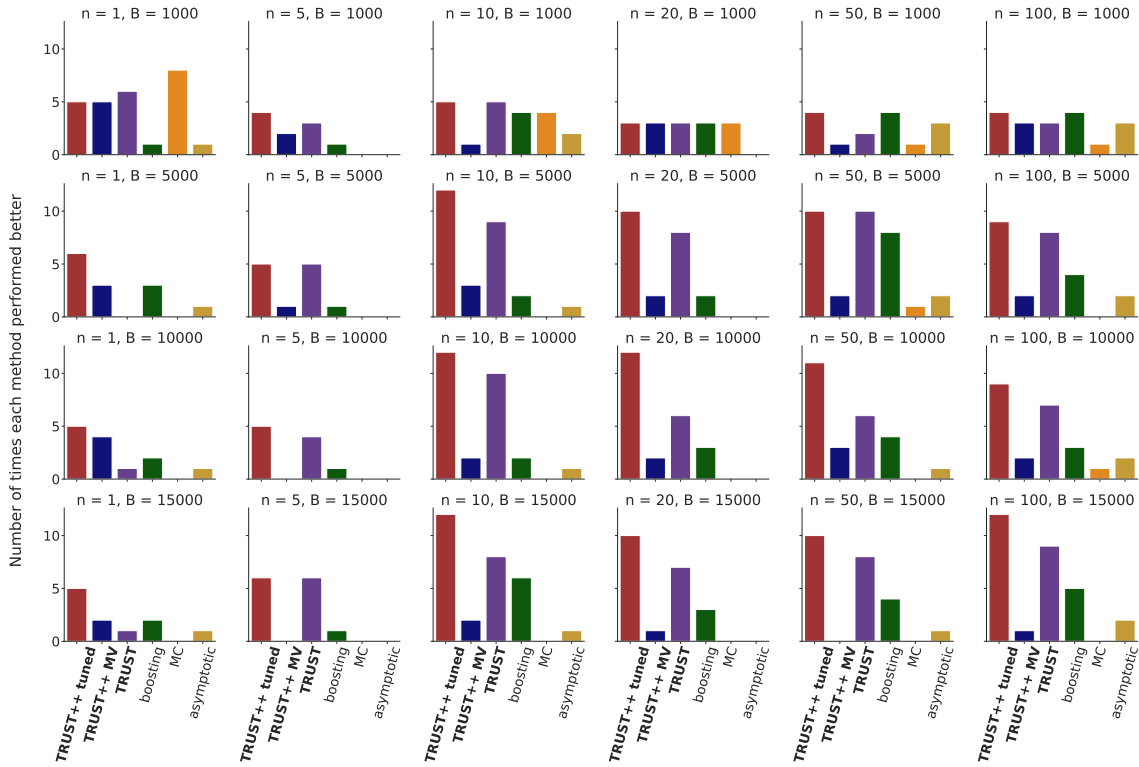


Figure 4: Frequency of times each method performed best (smallest significant MAE) for each statistic and likelihood model combination across different sample sizes  $n$  and simulation sizes  $B$ . Our methods are highlighted in bold. Overall, our methods demonstrated superior performance compared to other competing approaches in small sample settings, such as  $n = 1$ ,  $n = 5$ , and  $n = 10$ , while maintaining competitive performance for larger sample sizes, such as  $n = 50$  and  $n = 100$ .

- Figure 4 shows that tuned TRUST++ consistently outperforms all competing methods across  $B$  from 5000 to 15000 and for all  $n$ . Additionally, Figure 5 highlights the precision and reliability of tuned TRUST++ in achieving conditional coverage. Tuned TRUST++ maintains a high proportion of scenarios with strictly bounded MAE while showcasing lower loss than other competing approaches.
- TRUST exhibit strong performances for  $n \geq 5$ , showing a higher count of scenarios with superior outcomes across each combination of  $n$  and  $B$ , as illustrated in Figure 4. Similar to tuned TRUST++, TRUST also exhibits consistency in achieving conditional coverage, as evidenced in Figure 5.
- Both Monte-Carlo and Asymptotic methods present poor performance when the simulation budget exceeds 1000 and display an inconsistent control over conditional coverage as evidenced by Figures 4 and 5. Notably, Figure 5 illustrates that the asymptotic method only achieves lower loss values than other approaches in scenarios where it has a low proportion of cases with controlled MAE.

- Although the boosting method demonstrates competitive coverage consistency and strong performance in certain scenarios and specific combinations of  $n$  and  $B$ , as visualized in Figures 4 and 5, it is clear that this method is generally outperformed by TRUST and tuned TRUST++ in the majority of cases, and also display higher loss in instances where MAE bounds are tighter.
- Although TRUST++ MV does not match the performance of the tuned TRUST++ and TRUST, it demonstrates strong coverage consistency and performs well in certain scenarios, as shown in Figures 4 and 5.

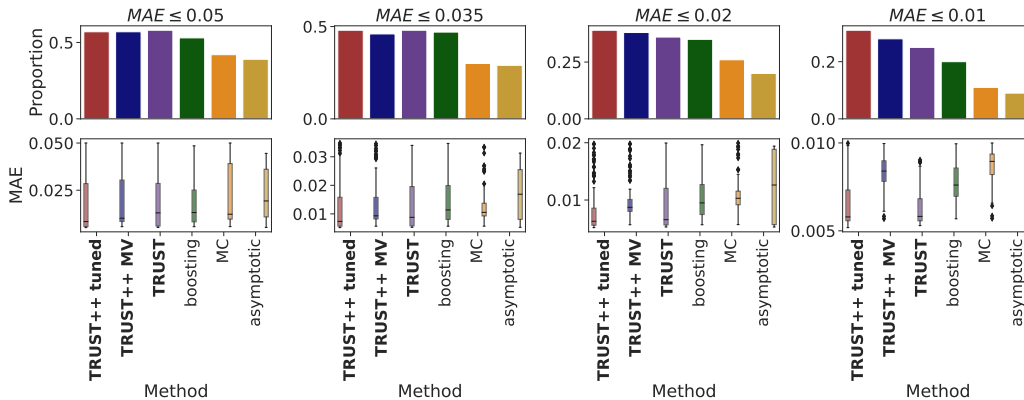


Figure 5: **Top:** Frequency of scenarios where each method achieves an MAE below varying fixed thresholds. Notably, as the threshold tightens, our methods continue to exhibit a high count of scenarios with minimal coverage errors. **Bottom:** Boxplot of MAE for each scenario with error values below the fixed thresholds. As the threshold decreases, both TRUST and TRUST++ demonstrate distinctly lower MAE values compared to competing methods. For comparability, only scenarios permitting asymptotic cutoff derivations were considered.

Based on all comparisons, we conclude that our framework consistently outperforms competing approaches in terms of conditional coverage for several settings.

## 5.2 Likelihood-free Inference Problems

We now apply our methods to construct confidence sets across 5 known LFI benchmarks, where the likelihood is intractable or no analytical formula exists for certain statistics, requiring them to be estimated. In cases of intractable likelihood, we simulate the data  $\mathbf{X} = (X_1, \dots, X_n)$  using a high-fidelity simulator  $F_\theta$ . Given a fixed  $\theta$ , we also assume that each  $X_i$  is i.i.d. The simulators and models are:

- **SLCP (Simple likelihood complex posterior):** in this model, we consider that  $\mathbf{x} = (\mathbf{x}_1, \mathbf{x}_2, \mathbf{x}_3, \mathbf{x}_4) \in \mathbb{R}^8$  represents 2d-coordinates of 4 points. The coordinates of each point are sampled independently from a multivariate Gaussian whose mean and covariance matrix are parametrized by a 5-dimensional parameter  $\theta$  (Hermans et al., 2021). Despite the likelihood’s simplicity, the posterior of this model is complex (Papamakarios et al., 2019), making it difficult to use the BFF and E-value statistics

in the analytical formula. We let  $\Theta = (-3, 3)^5$  and use  $\theta_i \sim U(-3, 3)$  as a prior for the model and to estimate  $\tau$ .

- **Two Moons:** here we consider a likelihood model with  $\mathbf{x} = (x_1, x_2) \in \mathbb{R}^2$  and a two-dimensional  $\theta$  such that the posterior exhibits a bimodal moon shape-like structure (Greenberg et al., 2019). In this case, we must model and approximate the posterior to estimate the BFF and E-value statistics. We set  $\Theta = (-1, 1)^2$  and use  $\theta_i \sim U(-1, 1)$  as a prior for the model and to estimate  $\tau$ .
- **M/G/1:** this model describes a processing and arrival queue system, where a 3-dimensional parameter  $\theta$  influences both the service time per customer and the intervals between arrivals (Hermans et al., 2021). Here, the sample  $\mathbf{x} = (x_1, \dots, x_5) \in \mathbb{R}^5$  consists of 5 equally spaced quantiles of inter-departure times. In this case, the likelihood  $\mathcal{L}(\mathbf{x}; \theta)$  is intractable, and computing the BFF and E-value statistics through likelihood-based inference would require high-dimensional integration (Blum and François, 2010). We set  $\Theta = (0, 10)^2 \times (0, 1/3)$  and use  $(\theta_1, \theta_2, \theta_3) \sim U(0, 10)^2 \times U(0, 1/3)$  as prior for the model and to estimate  $\tau$ .
- **Weinberg:** this simulator consists of a high-energy particle collision physics model (Hermans et al., 2021). Here, our sample  $\mathbf{x} \in \mathbb{R}$  is a measure of the Weinberg angle and we are interested in inferring the Fermi’s constant  $\theta \in \mathbb{R}$ . As the likelihood is intractable, we must estimate all kinds of statistics for this problem. We set  $\Theta = (0.5, 1.5)$ , and use the prior distribution  $\theta \sim U(0.5, 1.5)$  for estimating  $\tau$ .
- **SIR:** In this example, we examine an epidemiological model that tracks the dynamics of individuals across three states: susceptible (S), infectious (I), and recovered or deceased (R) (Lueckmann et al., 2021). The sample  $\mathbf{x} = (x_1, x_2, x_3) \in \mathbb{R}^3$  represents the count of individuals in each state within a population of 1000, observed after 10 iterations of the model. The parameter  $\theta$ , a 2-dimensional vector, denotes the contact rate and the mean recovery rate of the model. This case also involves an intractable likelihood, requiring estimation of all relevant statistics. We set  $\Theta = (0, 0.5)^2$  and apply the prior  $\theta_i \sim U(0, 0.5)$  for estimating  $\tau$ .

For choices of  $\tau$ , we consider both the E-value and BFF introduced in Section 5.1 along with the Waldo statistic (Masserano et al., 2023):

$$\text{Waldo}(\mathbf{x}, \theta_0) = (\mathbb{E}[\theta|\mathbf{x}] - \theta_0)^T \mathbb{V}[\theta|\mathbf{x}]^{-1} (\mathbb{E}[\theta|\mathbf{x}] - \theta_0), \quad (17)$$

where  $\mathbb{E}[\theta|\mathbf{x}]$  and  $\mathbb{V}[\theta|\mathbf{x}]$  replace the MLE estimator  $\hat{\theta}$  and its variance by the conditional mean and covariance matrix of  $\theta$  given  $\mathbf{x}$ . As detailed by Masserano et al. (2023), under Bayes estimator assumptions, the Waldo statistic retains the same asymptotic properties as the Wald statistic. However, for smaller  $n$ , Waldo can leverage consistent priors on  $\theta$  to produce tighter confidence sets. This makes Waldo a compelling choice in scenarios where the likelihood is intractable.

Since an exact posterior  $f(\theta|\mathbf{x})$  is unavailable for all statistics in the likelihood-free inference (LFI) context, we estimate posterior quantities using a Neural Posterior Estimator based on normalizing flows (Rezende and Mohamed, 2015; Hermans et al., 2021). This

method approximates the posterior  $f(\theta|\mathbf{x})$  through an amortized estimator  $\hat{f}_\psi(\theta|\mathbf{x})$ , constructed with neural network-based bijective transformations parameterized by  $\psi$  (Rezende and Mohamed, 2015). The estimator is trained on a simulated sample  $\{(\theta_1, \mathbf{X}_1), \dots, (\theta_B, \mathbf{X}_B)\}$  generated from each model or simulator. Details of normalizing flow architecture, implementation, and simulation budgets are given in Appendix A.

For each statistic and simulator, we evaluate all methods across combinations of  $n \in \{1, 5, 10, 20\}$  and  $B \in \{10, 15, 20, 30\} \times 10^3$ , increasing the simulation budgets relative to Section 5.1 to account for the greater complexity of these problems. Figure 6 summarizes the overall performance of each method, while Figure 7 illustrates the coverage control achieved by each method under different error thresholds. The results again reveal several performance distinctions among the methods:

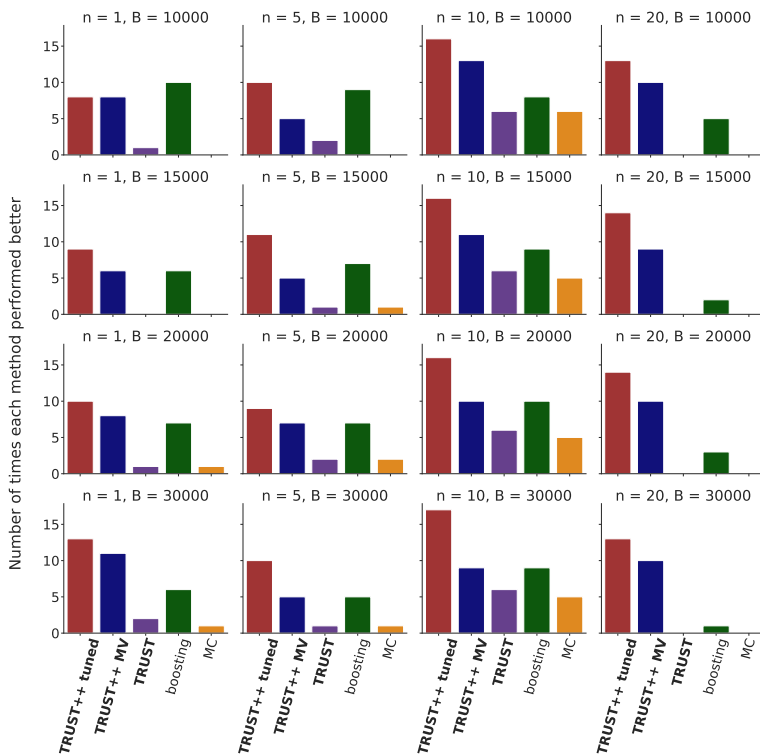


Figure 6: Frequency of times each method performed best for each statistic and simulator combination across different sample sizes  $n$  and simulation sizes  $B$ . Our methods are highlighted in bold. Overall, TRUST++ consistently demonstrated superior performance across all scenarios with a simulation budget exceeding 10000, while also maintaining competitive results for  $B = 10000$ .

- For  $n = 1$  and  $5$  with simulation budgets below 30000, Figure 6 shows a relatively balanced performance between tuned TRUST++, TRUST++ MV, and boosting. However, in all scenarios with  $n = 10$  or  $20$ , tuned TRUST++ consistently achieves superior results, with TRUST++ MV performing strongly and both outperforming boosting.



This suggests that our Breiman distance approach for computing local cutoffs adapts effectively to likelihood-free settings as sample sizes and simulation budgets increase.

- Figure 4 demonstrates that tuned TRUST++ consistently outperforms competing methods in nearly all scenarios (15 out of 16). Furthermore, Figure 7 highlights the precision and reliability of tuned TRUST++ in achieving conditional coverage even in likelihood-free scenarios, mirroring its strong performance observed in tractable experiments. Again, tuned TRUST++ consistently exhibits a high count of combinations with tightly bounded MAE and lower overall loss compared to all other approaches.
- The Monte Carlo method performs poorly across nearly all scenarios, showing weaker coverage control than other methods, as illustrated in Figures 6 and 7. These results highlight the limitations of the Monte Carlo method in adapting to likelihood-free scenarios.
- The boosting method demonstrates competitive coverage control and consistent performance in several scenarios, notably outperforming in the specific case of  $n = 1$  and  $B = 10000$ , as shown in Figures 4 and 5. However, in most cases, it is outperformed by both tuned TRUST++ and TRUST++ MV. Aligned with results from tractable experiments, the boosting method also exhibits higher loss under tighter MAE bounds compared to tuned TRUST++ in the likelihood-free context.

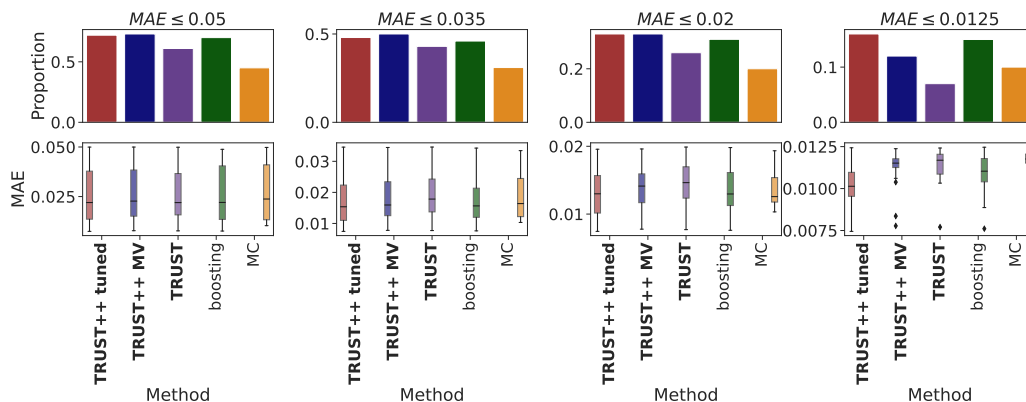


Figure 7: **Top:** Frequency of LFI scenarios where each method achieves an MAE below varying fixed thresholds. Particularly, as the threshold diminishes, TRUST++ continues to exhibit a high count of scenarios with minimal coverage errors. **Bottom:** Boxplot of MAE for each scenario with error values below the fixed thresholds. As the threshold decreases, TRUST++ presents a lower MAE distribution compared to all other approaches.

- Despite exhibiting poorer coverage control than boosting and tuned TRUST++, TRUST++ MV still shows strong performance across all scenarios, particularly standing out in cases with  $n = 20$ . This highlights the effective adaptation of the Majority-Vote scheme for computing local cutoffs within likelihood-free contexts.
- In contrast to the results seen in tractable experiments, TRUST demonstrates subpar performance and coverage control compared to both boosting and TRUST++ in

likelihood-free scenarios, as shown in Figures 6 and 7. This indicates that the TRUST partition requires enhancements for likelihood-free contexts, a need effectively addressed through the ensembling approach used in TRUST++.

From these experiments, we conclude that even in challenging likelihood-free examples, TRUST++ excels in achieving conditional coverage.

Figure 8 further illustrates the application of each method, showcasing the confidence regions alongside TRUST++’s uncertainty quantification for a specific realization of the two moons example. Both TRUST++ and boosting closely approximate the oracle region, whereas the Monte Carlo method significantly underestimates the region’s size. While TRUST++ and boosting produce similar confidence regions, TRUST++ distinguishes itself by offering an additional layer of uncertainty quantification. This uncertainty layer reveals insights into oracle information that may not be fully captured by the region estimators, likely due to constraints in the simulation budget.

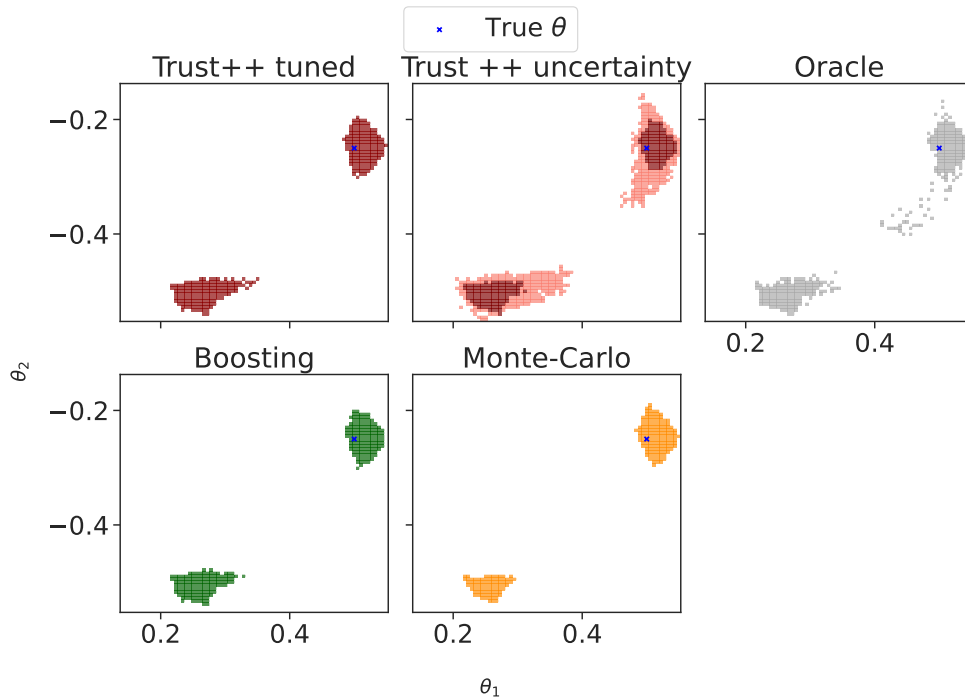


Figure 8: Visualization of 95% confidence regions and TRUST++ uncertainty for the two moons example, utilizing the e-value statistic with  $n = 20$  and  $B = 15000$ . In the uncertainty panel, the maroon areas represent regions where TRUST++ exhibits high confidence, while the salmon areas indicate regions with uncertainty. TRUST++ not only closely approximates the oracle set but also captures additional oracle information through its uncertainty regions, offering valuable insights into the precision of the cutoff estimation relative to the simulation budget. The user may choose to increase the number of simulations to decrease the uncertain region.

### 5.3 Examples of nuisance-parameter problems

In this section, we demonstrate the application of both of our methods in scenarios involving nuisance parameters. We begin with a Poisson counting experiment, originally introduced by [Dalmaso et al. \(2021\)](#) as an example from high-energy physics, where the BFF statistic is non-invariant, requiring both estimation and marginalization. Next, we tackle a classic inference problem: estimating parameter intervals within a gamma generalized linear model (GLM) under the presence of nuisance parameters and limited sample sizes. We compare our methods to the commonly used asymptotic approach, employing a likelihood ratio statistic that is marginalized over the nuisance parameter ([McCullagh, 2019](#)).

#### 5.3.1 POISSON COUNTING EXPERIMENT

We consider the observed data  $\mathbf{X} = (N_b, N_s)$  which consists of two counts where  $N_b \sim \text{Pois}(\nu\tau b)$  and  $N_s \sim \text{Pois}(\nu b + \mu s)$ . In this example,  $b$ ,  $s$ , and  $\tau$  are fixed hyperparameters, while  $\mu$  is the parameter of interest and  $\nu$  is the nuisance parameter. We define  $\theta = (\mu, \nu) \in \Theta = (0, 5) \times (0, 1.5)$  and fix the hyper-parameters as  $s = 15$ ,  $b = 70$  and  $\tau = 1$  to avoid the Gaussian limiting regime for Poisson distributions. We also take the uniform distribution over the parameter space as prior. To derive a statistic  $\tau(\mathbf{X}, \mu)$  in this case, in this context, we use a marginalized BFF statistic based on the posterior  $f(\mu|\mathbf{x})$ , estimated through a normalizing flows approach (details in Appendix A). We set the simulation budget to  $B = 10 \times 10^3$  and  $n = 1$  to fit all methods.

Although the BFF statistic is marginalized over nuisance parameters, it may still depend on their values. Therefore, we fit all methods considering the full parameter  $(\mu, \nu)$  and compute the cutoff for  $\mu$  through Eq. 7. Our approaches facilitate this computation by using the tree structure and achieve better results, as shown in Table 1.

Table 1: Mean absolute coverage deviation from the oracle for each method in the Poisson counting example. The average across 15 runs is reported along with twice its standard error. TRUST++ demonstrates exceptional performance.

Methods	$d_\alpha$	$SE \cdot 2$
TRUST	0.0369	$0.14 \cdot 10^{-4}$
TRUST++	0.0041	$0.15 \cdot 10^{-4}$
Boosting	0.0084	$0.12 \cdot 10^{-4}$
MC	0.1460	$0.11 \cdot 10^{-4}$

Table 1 highlights the strong performance of TRUST++, with coverage closely aligning with the oracle, emphasizing its adaptability to challenges involving nuisance parameters. Also, we observe that the Monte Carlo method shows a substantial deviation from the oracle, further illustrating its limitations in adapting effectively to different inference scenarios.

While TRUST++ achieves the best results, boosting also performs well, providing coverage that is similarly close to the oracle’s. Figure 9 details the differences between the methods. We observe that TRUST++ effectively controls coverage deviation across all combinations of  $(\mu, \nu)$ . In contrast, boosting exhibits areas of higher deviation, particularly around  $\mu = 2$  for all values of  $\nu$  and around  $\mu = 3$  when  $\nu$  is low. This demonstrates TRUST++’s accuracy in

approximating the oracle region throughout the parameter space, indicating its effectiveness in estimating the cutoff  $C_\mu$  defined in Eq. 7.

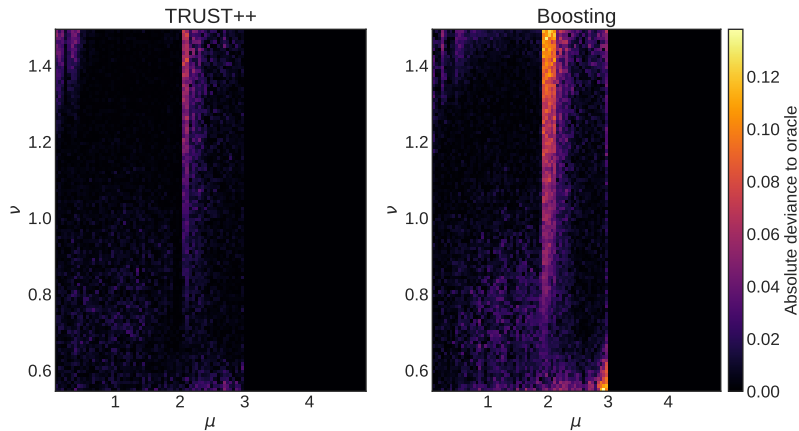


Figure 9: Comparison of absolute deviations from the oracle for each pair of parameters between TRUST++ and boosting. Notably, around  $\mu = 2$ , boosting exhibits significant deviations from the oracle, whereas TRUST++ effectively controls these deviations, keeping them below 0.1.

### 5.3.2 GAMMA GLM EXPERIMENT

Consider i.i.d data  $Y_i \in \mathbb{R}^+$  generated from a gamma generalized linear model (GLM) with fixed covariates  $\mathbf{X}_i = (X_{i,1}, X_{i,2}) \in (-1, 1)^2$ :

$$Y_i \sim \text{Gamma}(1/\phi, \phi \cdot \exp\{\beta_0 + \beta_1 X_{i,1} + \beta_2 X_{i,2}\}) , \quad (18)$$

where  $\phi$  is the dispersion parameter and  $\beta_0, \beta_1$  and  $\beta_2$  are coefficients for the linear predictor, with  $\phi \in (0, 1.75)$  and  $\boldsymbol{\beta} = (\beta_0, \beta_1, \beta_2) \in \mathbb{R}^3$ . The expected value of each  $Y_i$  is given by:

$$\mathbb{E}[Y_i] = \exp\{\beta_0 + \beta_1 X_1 + \beta_2 X_2\} .$$

A standard problem in this setting is to derive a valid confidence interval for a single parameter  $\beta_j$ . A widely used approach is to construct an asymptotic confidence interval based on the marginalized likelihood ratio statistic:  $LR(\mathbf{y}, \beta_j) = \log \mathcal{L}(\mathbf{y}; \hat{\boldsymbol{\beta}}_{-j}, \beta_j) - \log \mathcal{L}(\mathbf{y}; \hat{\boldsymbol{\beta}})$ , where  $\hat{\boldsymbol{\beta}}$  is the MLE,  $\hat{\boldsymbol{\beta}}_{-j}$  the MLE restricted under a fixed  $\beta_j$  and  $\mathcal{L}(\cdot; \boldsymbol{\beta})$  denotes the GLM likelihood as defined in Eq. 18. Using this statistic, an asymptotic confidence interval can be easily derived by referencing the  $\chi_1^2$  distribution to compute  $C_{\beta_j}$  in a invariant way.

The limitation of this approach is that it relies on large sample sizes to be effective; for small samples, it may fail to produce a valid confidence interval, as illustrated in Figure 1(b). This is because the marginalized likelihood ratio statistic still depends on the remaining nuisance parameters,  $\boldsymbol{\beta}_{-j}$  and  $\phi$  in low-sample regimes. This limitation can be addressed with our approach by computing  $C_{\beta_j}$  using Eq. 7 in a scalable manner. To apply all simulation-based approaches, we assume the priors  $\boldsymbol{\beta} \sim N(0, 4) \cdot N(0, 1)^2$  and

$\phi \sim \text{Truncated Exponential}(1, 1.75)$ . For method comparison, we set the parameter of interest to  $j = 1$ , the sample size to  $n = 50$  and the simulation budget to  $B = 10 \cdot 10^3$ , with the covariate matrix  $\mathbf{X}$  fixed according to values generated independently from  $U(-1, 1)^2$ . Table 2 shows the mean deviation from the oracle coverage for each method, while Figure 1 illustrates the probability of coverage and confidence intervals for specific values of  $\beta_j$  and  $\mathbf{Y}$  samples.

Table 2: Mean absolute coverage deviation from the oracle for each method in the GLM example. The average across 15 runs is reported along with twice its standard error. TRUST++ demonstrates superior performance compared to all competing methods.

Methods	$d_\alpha$	$SE \cdot 2$
TRUST	0.0312	$0.176 \cdot 10^{-3}$
TRUST++	0.0157	$0.163 \cdot 10^{-3}$
Boosting	0.0234	$0.171 \cdot 10^{-3}$
MC	0.0207	$0.157 \cdot 10^{-3}$
Asymptotic	0.0327	$0.171 \cdot 10^{-3}$

By Table 2 we notice that TRUST++ achieves the best performance, with coverage closely matching the oracle and outperforming Monte Carlo and boosting by a large margin. Figure 1 illustrate this proximity for specific values of  $\beta_j$  and observed sample values  $\mathbf{Y}$ . Although TRUST++ exhibits overcoverage relative to the nominal level  $1 - \alpha$  and produces larger confidence intervals compared to other methods, it closely emulates the oracle’s behavior, making it more valid than the competing approaches. Additionally, TRUST++’s uncertainty bar indicates that for nearly all parameters within the confidence interval, we can be confident they truly lie within the interval, reflecting a well-estimated range. Furthermore, both Table 2 and Figure 1 reveal that the asymptotic approach not only deviates more from the oracle but also undercovers and underestimates the confidence interval length. This underscores the limitations of asymptotic methods for small sample sizes and nuisance parameter, even in problems with tractable likelihoods.

## 6 Final Remarks

This paper introduces novel methods, TRUST and TRUST++, for the distribution-free calibration of statistical confidence sets, ensuring both finite-sample local coverage and asymptotic conditional coverage. By leveraging tools from conformal inference, we create robust confidence sets that extend the applicability of traditional conformal techniques, typically used for generating prediction intervals, to the domain of statistical inference. This adaptation allows us to maintain the desired coverage properties even in challenging settings. In practice, this translates to superior performances across a variety of scenarios, particularly in cases involving small sample sizes  $n$  and larger simulation budgets  $B$ .

Furthermore, our methods effectively address inference settings with nuisance parameters, a notable challenge for other approaches, especially in likelihood-free inference. Unlike existing techniques, TRUST and TRUST++ also enable robust uncertainty quantification about the oracle confidence sets, providing valuable insights into whether additional simulated data is needed to achieve more reliable estimates.

Theorem 3 demonstrates that both TRUST and TRUST++ are consistent estimators for quantile regression with respect to any random variable in  $\mathbf{x}$ . While we applied these methods specifically to quantile-regress the conformal score on  $\mathbf{x}$ , their utility extends far beyond this particular setting. They can be applied in a variety of contexts, such as constructing predictive intervals in a prediction setting, including for multivariate  $Y$ . This capability allows for the generation of label-conditional predictive sets that aim to control  $\mathbb{P}(Y \in \mathbb{R}(\mathbf{X}) \mid Y = y)$ , ensuring coverage conditional on the label.

To our knowledge, no other conformal methods aim to control label-conditional coverage for continuous outcomes  $Y$ , making this a novel contribution to the field. This work paves the way for future research to explore label-conditional inference in complex, continuous and multivariate-label settings, potentially improving the reliability of prediction intervals in domains where conditional control is critical.

### Acknowledgments and Disclosure of Funding

L.M.C.C is grateful for the fellowship provided by São Paulo Research Foundation (FAPESP), grant 2022/08579-7. R. I. is grateful for the financial support of FAPESP (grants 2019/11321-9 and 2023/07068-1) and CNPq (grants 422705/2021-7 and 305065/2023-8). R. B. S. produced this work as part of the activities of Fundação de Amparo à Pesquisa do Estado de São Paulo Research, Innovation and Dissemination Center for Neuromathematics (grant 2013/07699-0). The authors are also grateful to Rodrigo F. L. Lassance and Ann B. Lee for their suggestions and insightful discussions.

## References

- Sara Algeri, Jelle Aalbers, Knut Dundas Morå, and Jan Conrad. Searching for new physics with profile likelihoods: Wilks and beyond. *arXiv preprint arXiv:1911.10237*, 2019.
- Anastasios N Angelopoulos, Stephen Bates, et al. Conformal prediction: A gentle introduction. *Foundations and Trends® in Machine Learning*, 16(4):494–591, 2023.
- Meili Baragatti, Bertrand Cloez, David Métivier, and Isabelle Sanchez. Approximate bayesian computation with deep learning and conformal prediction. *arXiv preprint arXiv:2406.04874*, 2024.
- Nathan Berg. No-decision classification: an alternative to testing for statistical significance. *the Journal of socio-Economics*, 33(5):631–650, 2004.
- G erard Biau, Luc Devroye, and G abor Lugosi. Consistency of random forests and other averaging classifiers. *J. Mach. Learn. Res.*, 9:2015–2033, June 2008. ISSN 1532-4435.
- Michael GB Blum and Olivier Fran ois. Non-linear regression models for approximate bayesian computation. *Statistics and computing*, 20:63–73, 2010.
- Henrik Bostr m and Ulf Johansson. Mondrian conformal regressors. In *Conformal and Probabilistic Prediction and Applications*, pages 114–133. PMLR, 2020.
- Henrik Bostr m, Ulf Johansson, and Tuwe L fstr m. Mondrian conformal predictive distributions. In Lars Carlsson, Zhiyuan Luo, Giovanni Cherubin, and Khuong An Nguyen, editors, *Conformal and Probabilistic Prediction and Applications, 8-10 September 2021, Virtual Event*, volume 152 of *Proceedings of Machine Learning Research*, pages 24–38. PMLR, 2021. URL <https://proceedings.mlr.press/v152/bostrom21a.html>.
- Johann Brehmer, Gilles Louppe, Juan Pavez, and Kyle Cranmer. Mining gold from implicit models to improve likelihood-free inference. *Proceedings of the National Academy of Sciences*, 117(10):5242–5249, 2020.
- Leo Breiman. Random forests. *Machine learning*, 45:5–32, 2001.
- Luben Cabezas, Mateus P Otto, Rafael Izbicki, and Rafael B Stern. Regression trees for fast and adaptive prediction intervals. *arXiv preprint arXiv:2402.07357*, 2024.
- George Casella and Roger Berger. *Statistical inference*. CRC Press, 2024.
- Jiahua Chen and Pengfei Li. Hypothesis test for normal mixture models: The em approach. 2009.
- Kyle Cranmer, Johann Brehmer, and Gilles Louppe. The frontier of simulation-based inference. *Proceedings of the National Academy of Sciences*, 117(48):30055–30062, 2020.
- Niccolo Dalmaso, Rafael Izbicki, and Ann Lee. Confidence sets and hypothesis testing in a likelihood-free inference setting. In *International Conference on Machine Learning*, pages 2323–2334. PMLR, 2020.

- Niccolò Dalmaso, Luca Masserano, David Zhao, Rafael Izbicki, and Ann B Lee. Likelihood-free frequentist inference: Bridging classical statistics and machine learning in simulator-based inference. *arXiv preprint arXiv:2107.03920*, 2021.
- Carlos A de B Pereira, Julio Michael Stern, and Sergio Wechsler. Can a significance test be genuinely bayesian? *Bayesian Analysis*, 3(1):79–100, 2008.
- Morris H DeGroot and Mark J Schervish. Probability and statistics.[sl]. *Pearson Education*, 19:33, 2012.
- Victor Dheur, Tanguy Bosser, Rafael Izbicki, and Souhaib Ben Taieb. Distribution-free conformal joint prediction regions for neural marked temporal point processes. *arXiv preprint arXiv:2401.04612*, 2024.
- Marcio Diniz, Carlos AB Pereira, Adriano Polpo, Julio M Stern, and Sergio Wechsler. Relationship between bayesian and frequentist significance indices. *International Journal for Uncertainty Quantification*, 2(2), 2012.
- Mathias Drton. Likelihood ratio tests and singularities. 2009.
- Conor Durkan, Artur Bekasov, Iain Murray, and George Papamakarios. Neural spline flows. *Advances in neural information processing systems*, 32, 2019.
- Luís G Esteves, Rafael Izbicki, Julio M Stern, and Rafael B Stern. The logical consistency of simultaneous agnostic hypothesis tests. *Entropy*, 18(7):256, 2016.
- Yoav Freund and Robert E Schapire. A decision-theoretic generalization of on-line learning and an application to boosting. *Journal of computer and system sciences*, 55(1):119–139, 1997.
- David Greenberg, Marcel Nonnenmacher, and Jakob Macke. Automatic posterior transformation for likelihood-free inference. In *International Conference on Machine Learning*, pages 2404–2414. PMLR, 2019.
- Leying Guan. Localized conformal prediction: A generalized inference framework for conformal prediction. *Biometrika*, 110(1):33–50, 2023.
- Gerald J Hahn and William Q Meeker. *Statistical intervals: a guide for practitioners*, volume 92. John Wiley & Sons, 2011.
- Trevor Hastie, Robert Tibshirani, Jerome H Friedman, and Jerome H Friedman. *The elements of statistical learning: data mining, inference, and prediction*, volume 2. Springer, 2009.
- Joeri Hermans, Arnaud Delaunoy, François Rozet, Antoine Wehenkel, Volodimir Begy, and Gilles Louppe. A trust crisis in simulation-based inference? your posterior approximations can be unfaithful. *arXiv preprint arXiv:2110.06581*, 2021.
- Rohan Hore and Rina Foygel Barber. Conformal prediction with local weights: randomization enables local guarantees. *arXiv preprint arXiv:2310.07850*, 2023.



- R. Izbicki, A.B. Lee, and C.M. Schafer. High-dimensional density ratio estimation with extensions to approximate likelihood computation. *Journal of Machine Learning Research (AISTATS Track)*, pages 420–429, 2014.
- Rafael Izbicki, Ann B Lee, and Taylor Pospisil. ABC–CDE: Toward approximate bayesian computation with complex high-dimensional data and limited simulations. *Journal of Computational and Graphical Statistics*, 28(3):481–492, 2019.
- Rafael Izbicki, Gilson Shimizu, and Rafael Stern. Flexible distribution-free conditional predictive bands using density estimators. In *International Conference on Artificial Intelligence and Statistics*, pages 3068–3077. PMLR, 2020.
- Rafael Izbicki, Gilson Shimizu, and Rafael B Stern. Cd-split and hpd-split: Efficient conformal regions in high dimensions. *Journal of Machine Learning Research*, 23(87):1–32, 2022.
- Rafael Izbicki, Luben M. C. Cabezas, Fernando A. B. Colugnatti, Rodrigo F. L. Lassance, Altay A. L. de Souza, and Rafael B. Stern. React to nhst: Sensible conclusions to meaningful hypotheses. 2023. URL <https://arxiv.org/abs/2308.09112>.
- Jef Jonkers, Glenn Van Wallendael, Luc Duchateau, and Sofie Van Hoecke. Conformal predictive systems under covariate shift. *arXiv preprint arXiv:2404.15018*, 2024.
- Robert E Kass and Adrian E Raftery. Bayes factors. *Journal of the american statistical association*, 90(430):773–795, 1995.
- Erich Leo Lehmann, Joseph P Romano, and George Casella. *Testing statistical hypotheses*, volume 3. Springer, 1986.
- Jing Lei and Larry Wasserman. Distribution-free prediction bands for non-parametric regression. *Journal of the Royal Statistical Society Series B: Statistical Methodology*, 76(1):71–96, 2014.
- Jan-Matthis Lueckmann, Giacomo Bassetto, Theofanis Karaletsos, and Jakob H Macke. Likelihood-free inference with emulator networks. In *Symposium on Advances in Approximate Bayesian Inference*, pages 32–53, 2019.
- Jan-Matthis Lueckmann, Jan Boelts, David Greenberg, Pedro Goncalves, and Jakob Macke. Benchmarking simulation-based inference. In *International conference on artificial intelligence and statistics*, pages 343–351. PMLR, 2021.
- George Marsaglia, Wai Wan Tsang, and Jingbo Wang. Evaluating kolmogorov’s distribution. *Journal of statistical software*, 8:1–4, 2003.
- Luca Masserano, Tommaso Dorigo, Rafael Izbicki, Mikael Kuusela, and Ann Lee. Simulator-based inference with waldo: Confidence regions by leveraging prediction algorithms and posterior estimators for inverse problems. In *International Conference on Artificial Intelligence and Statistics*, pages 2960–2974. PMLR, 2023.
- Peter McCullagh. *Generalized linear models*. Routledge, 2019.

- Nicolai Meinshausen and Greg Ridgeway. Quantile regression forests. *Journal of machine learning research*, 7(6), 2006.
- George Papamakarios, David Sterratt, and Iain Murray. Sequential neural likelihood: Fast likelihood-free inference with autoregressive flows. In *The 22nd International Conference on Artificial Intelligence and Statistics*, pages 837–848, 2019.
- Yash Patel, Declan McNamara, Jackson Loper, Jeffrey Regier, and Ambuj Tewari. Variational inference with coverage guarantees in simulation-based inference. In *Forty-first International Conference on Machine Learning*, 2024.
- Fabian Pedregosa, Gaël Varoquaux, Alexandre Gramfort, Vincent Michel, Bertrand Thirion, Olivier Grisel, Mathieu Blondel, Peter Prettenhofer, Ron Weiss, Vincent Dubourg, et al. Scikit-learn: Machine learning in python. *the Journal of machine Learning research*, 12:2825–2830, 2011.
- Carlos Alberto de Bragança Pereira and Julio Michael Stern. Evidence and credibility: full bayesian significance test for precise hypotheses. *Entropy*, 1(4):99–110, 1999.
- Danilo Rezende and Shakir Mohamed. Variational inference with normalizing flows. In *International conference on machine learning*, pages 1530–1538. PMLR, 2015.
- Mauricio Sadinle, Jing Lei, and Larry Wasserman. Least ambiguous set-valued classifiers with bounded error levels. *Journal of the American Statistical Association*, 114(525): 223–234, 2019.
- Mark J Schervish. *Theory of statistics*. Springer Science & Business Media, 2012.
- Glenn Shafer and Vladimir Vovk. A tutorial on conformal prediction. *Journal of Machine Learning Research*, 9(3), 2008.
- Vincent Stimper, David Liu, Andrew Campbell, Vincent Berenz, Lukas Ryll, Bernhard Schölkopf, and José Miguel Hernández-Lobato. normflows: A pytorch package for normalizing flows. *Journal of Open Source Software*, 8(86):5361, 2023. doi: 10.21105/joss.05361. URL <https://doi.org/10.21105/joss.05361>.
- Aad W Van der Vaart. *Asymptotic statistics*, volume 3. Cambridge university press, 2000.
- Vladimir Vovk, Alexander Gammerman, and Glenn Shafer. *Algorithmic learning in a random world*, volume 29. Springer, 2005.
- Vladimir Vovk, Ivan Petej, and Valentina Fedorova. From conformal to probabilistic prediction. In *Artificial Intelligence Applications and Innovations: AIAI 2014 Workshops: CoPA, MHDW, IIVC, and MT4BD, Rhodes, Greece, September 19-21, 2014. Proceedings 10*, pages 221–230. Springer, 2014.
- Vladimir Vovk, Valentina Fedorova, Ilia Nouretdinov, and Alexander Gammerman. Criteria of efficiency for conformal prediction. In *Conformal and Probabilistic Prediction with Applications: 5th International Symposium, COPA 2016, Madrid, Spain, April 20-22, 2016, Proceedings 5*, pages 23–39. Springer, 2016.

Vladimir Vovk, Jieli Shen, Valery Manokhin, and Min-ge Xie. Nonparametric predictive distributions based on conformal prediction. *Mach. Learn.*, 108(3):445–474, 2019. doi: 10.1007/S10994-018-5755-8.

Vladimir Vovk, Ivan Petej, Iliia Nouretdinov, Valery Manokhin, and Alexander Gamerman. Computationally efficient versions of conformal predictive distributions. *Neurocomputing*, 397:292–308, 2020. doi: 10.1016/J.NEUCOM.2019.10.110.

Supawadee Wichitchan, Weixin Yao, and Guangren Yang. Hypothesis testing for finite mixture models. *Computational statistics & data analysis*, 132:180–189, 2019.

## Appendix A. Experiment details

For all experiments involving the application of normalizing flows for posterior estimation, we utilized the *normflows* Python package (Stimper et al., 2023). Specifically, we employed the autoregressive rational quadratic spline architecture for each flow (Durkan et al., 2019). All models were trained on an ACER Nitro 5 AN515-54 using GPU (cuda). The architectural details for both the LFI examples and the nuisance parameter experiment are outlined below.

### A.1 LFI posterior estimator

In the LFI setting, we employed a total of six flows, each consisting of two hidden layers with 128 units per layer. A dropout probability of 0.35 was applied to each layer to prevent overfitting. For optimization, we trained the model for a maximum of 1000 epochs, with early stopping triggered after 30 epochs of no improvement. The Adam optimizer was used with a learning rate of  $3 \times 10^{-4}$  and a weight decay of  $1 \times 10^{-5}$ . To train the neural network, we simulated  $B = 30,000$  samples for all sample sizes  $n$ .

### A.2 Poisson Counting Experiment posterior estimator

For the nuisance parameter experiment, we used a total of four flows with the same configuration for hidden layers, hidden units, dropout probability, and optimizer as in the LFI neural posterior model. In this case, training was conducted for up to 2000 epochs, with early stopping triggered after 200 epochs without improvement. The neural network was trained using  $B = 25,000$  simulated samples for  $n = 1$ .

## Appendix B. Algorithm for tuning $M$

---

### Algorithm 3: Tuning algorithm for $M$

---

**Data:** Validation grid size  $B_{\text{tune}}$ ; grid of  $M$ 's between 0 to  $K$   $M_{\text{grid}}$ ; fitted TRUST++; number of simulated statistics  $n_{\text{sim}}$  in each grid point

**Result:** Tuned value of  $M$ ,  $M_{\text{tuned}}$

simulate  $\Theta_{\text{grid}} = (\theta_1, \dots, \theta_{B_{\text{tune}}})$  from the prior ;

**for**  $M_{\text{cand}} \in M_{\text{grid}}$  **do**

    compute  $\hat{C}_\theta$  in TRUST++ with  $M$  fixed as  $M_{\text{cand}}$  for each  $\theta \in \Theta_{\text{grid}}$  ;

    compute  $\text{cover}_\alpha(\hat{C}, \theta)$  for each  $\theta \in \Theta_{\text{grid}}$  (as in Eq. 10);

$MAE_{M_{\text{cand}}} \leftarrow MAE(\hat{C}, \alpha)$  (as in Eq. 11) ;

**end**

$M_{\text{tuned}} \leftarrow \arg \min_{M_{\text{cand}} \in M_{\text{grid}}} \{MAE_{M_{\text{cand}}}\}$  ;

**return**  $M_{\text{tuned}}$

---

## Appendix C. Proofs

### C.1 Section 2 - Methodology

**Proof** [Proof of Theorem 1] Notice that

$$\begin{aligned} \mathbb{P}(\theta \in \mathcal{I}(\mathbf{x}) | \theta \notin R(\mathbf{x})) &= \mathbb{P}\left(\tau(\mathbf{x}, \theta) \geq \widehat{C}_\theta^U | \tau(\mathbf{x}, \theta) \leq C_\theta\right) \\ &= \mathbb{P}\left(\widehat{C}_\theta^U \leq C_\theta | \tau(\mathbf{x}, \theta) \leq C_\theta\right) \leq \beta/2, \end{aligned}$$

which proves the first statement. The proof for the second statement is analogous. ■

### C.2 Section 3 - Theoretical Results

To summarize, in TRUST, the partition is created by building a regression tree that uses  $\theta$  as the input and  $\tau(\mathbf{x}, \theta)$  as the output. This tree, trained on the simulated data

$$\theta_1, \tau(\mathbf{X}_1, \theta_1), \dots, (\theta_B, \tau(\mathbf{X}_B, \theta_B)),$$

naturally induces a partition on  $\Theta$ .

For TRUST++, we extend this approach by generating  $K$  regression trees. We then use Breiman's proximity measure  $\rho(\theta', \theta)$ , which counts the number of times  $\theta'$  and  $\theta$  appear together in the same leaf across these  $K$  trees. Finally, we define the partition  $\mathcal{A}$  based on this proximity measure, using the equivalence relation  $\theta \sim \theta' \iff \rho(\theta', \theta) = K$ ; in other words,  $\theta$  and  $\theta'$  must appear together in the same leaves across all  $K$  trees.

This framework ensures that the partition  $\mathcal{A}$  meets the necessary structural conditions to apply conformal prediction as stated in Theorem 2.

**Proof** [Proof of Theorem 2] This is a straightforward application of conformal prediction (see Angelopoulos et al. (2023)). The complete proof can be found in detail in (Cabezas et al., 2024, Theorem 2). ■

To prove Theorem 3 we need the following lemma.

**Lemma 2** *Let  $H(t|\theta) = \mathbb{P}(\tau(\mathbf{X}, \theta) \leq t|\theta)$  and  $A$  be a measurable set. Suppose  $p(x, \theta)$  is the joint PDF of  $(\mathbf{X}, \theta)$ , satisfying  $\int p(x, \theta) dx = r(\theta) > 0$ . Then we have*

$$\mathbb{E}[H(t|\theta) | \theta \in A] = \mathbb{P}(\tau(\mathbf{X}, \theta) \leq t | \theta \in A).$$

**Proof** Define  $c := \mathbb{P}(\theta \in A)$ , the result follows from a straightforward calculation, as shown next.

$$\begin{aligned}
 \mathbb{E}[H(t|\theta)|\theta \in A] &= \frac{1}{\mathbb{P}(\theta \in A)} \mathbb{E}[H(t|\theta)\mathbb{I}[\theta \in A]] \\
 &= c^{-1} \int H(t|\theta)\mathbb{I}[\theta \in A]r(\theta)d\theta \\
 &= c^{-1} \int \mathbb{P}(\tau(\mathbf{X}, \theta) \leq t|\theta)\mathbb{I}[\theta \in A]r(\theta)d\theta \\
 &= c^{-1} \int \left( \frac{1}{r(\theta)} \int \mathbb{I}[\tau(x, \theta) \leq t]p(x, \theta)dx \right) \mathbb{I}[\theta \in A]r(\theta)d\theta \\
 &= c^{-1} \int \int \mathbb{I}[\tau(x, \theta) \leq t]\mathbb{I}[\theta \in A]p(x, \theta)dx d\theta \\
 &= c^{-1} \mathbb{P}(\tau(\mathbf{X}, \theta) \leq t, \theta \in A) \\
 &= \mathbb{P}(\tau(\mathbf{X}, \theta) \leq t | \theta \in A).
 \end{aligned}$$

■

Under the Assumption 1, for a sufficiently large  $B$ , we achieve  $H(t|\theta') \approx \widehat{H}_B(t|\theta')$ , for any  $\theta' \in \Theta$  and  $t \in \mathbb{R}$ . Based on this approximation, we outline here the intuition for how Theorem 3 will be established in detail later.

Specifically, for a fixed  $\theta$  of interest, by Lemma 2:

$$\begin{aligned}
 \mathbb{P}(\tau(\mathbf{X}, \theta') \leq t | \theta' \in A(\theta)) &= \mathbb{E}[H(t|\theta') | \theta' \in A(\theta)] \\
 &\approx \mathbb{E}[\widehat{H}_B(t|\theta') | \theta' \in A(\theta)],
 \end{aligned}$$

where the first equality results from a straightforward calculation, with its proof provided in the appendix.

By the construction of the partitions in TRUST and TRUST++, if  $\theta' \in A(\theta)$ , then  $\widehat{H}_B(t|\theta') = \widehat{H}_B(t|\theta)$ . Therefore,

$$\begin{aligned}
 \mathbb{P}(\tau(\mathbf{X}, \theta') \leq t | \theta' \in A(\theta)) &\approx \mathbb{E}[\widehat{H}_B(t|\theta') | \theta' \in A(\theta)] \\
 &= \mathbb{E}[\widehat{H}_B(t|\theta) | \theta' \in A(\theta)] \\
 &\approx \mathbb{E}[H(t|\theta) | \theta' \in A(\theta)] \\
 &= H(t|\theta).
 \end{aligned}$$

This implies that, as long as our approximation  $\widehat{H}_B$  closely matches  $H$ , our partition-based estimate will serve as a reliable approximation of the test statistics distribution. In particular, as discussed in Section 2.1.1, let  $\widehat{C}_{\theta, B} = \widehat{H}_B^{-1}(\alpha|\theta)$  denote the  $\alpha$ -quantile of the values  $\{\tau(\mathbf{X}_b, \theta_b) : b \in I_{A(\theta)}\}$ . Then,

$$\mathbb{P}\left(\theta \notin \widehat{R}_B(\mathbf{X})|\theta\right) = H(\widehat{C}_{\theta, B}|\theta) \approx \mathbb{P}(\tau(\mathbf{X}, \theta') \leq \widehat{C}_{\theta, B} | \theta' \in A(\theta)) = \alpha,$$

suggesting that our methods indeed should achieve optimal coverage.

**Proof** [Proof of Theorem 3]

Fix  $\theta$ . By Assumption 1, for any  $\varepsilon, \delta > 0$ , there exists  $B_0$  and a subset  $\Gamma \subset (\Theta \times \mathcal{X})^B$  such that  $\mathbb{P}(\Gamma) \geq 1 - \delta$  and, conditionally on  $\Gamma$ ,

$$\sup_{\tilde{t} \in \mathbb{R}, \tilde{\theta} \in \Theta} \left| \widehat{H}_B(\tilde{t}|\tilde{\theta}) - H(\tilde{t}|\tilde{\theta}) \right| \leq \varepsilon.$$

By Lemma 2,

$$\mathbb{P}(\tau(\mathbf{X}, \theta') \leq t | \theta' \in A(\theta)) = \mathbb{E}[H(t|\theta') | \theta' \in A(\theta)].$$

Conditionally on  $\Gamma$ , we know that

$$H(t|\theta') \geq \widehat{H}_B(t|\theta') - \varepsilon$$

holds uniformly for any possible value of  $\theta' \in \Theta, t \in \mathbb{R}$ . Thus,

$$\begin{aligned} \mathbb{P}(\tau(\mathbf{X}, \theta') \leq t | \theta' \in A(\theta), \Gamma) &= \mathbb{E}[H(t|\theta') | \theta' \in A(\theta), \Gamma] \\ &\geq \mathbb{E}[\widehat{H}_B(t|\theta') - \varepsilon | \theta' \in A(\theta), \Gamma] \\ &= \mathbb{E}[\widehat{H}_B(t|\theta') | \theta' \in A(\theta), \Gamma] - \varepsilon. \end{aligned}$$

Note that if  $\theta' \in A(\theta)$ , then  $A(\theta') = A(\theta)$ , hence  $\widehat{H}_B(t|\theta') = \widehat{H}_B(t|\theta)$ . Therefore,

$$\begin{aligned} \mathbb{P}(\tau(\mathbf{X}, \theta') \leq t | \theta' \in A(\theta), \Gamma) &\geq \mathbb{E}[\widehat{H}_B(t|\theta) | \theta' \in A(\theta), \Gamma] - \varepsilon \\ &= \mathbb{E}[\widehat{H}_B(t|\theta) | \theta' \in A(\theta), \Gamma] - \varepsilon. \end{aligned}$$

Using the fact that, conditionally on  $\Gamma$ ,

$$\widehat{H}_B(t|\theta) \geq H(t|\theta) - \varepsilon,$$

we obtain

$$\begin{aligned} \mathbb{P}(\tau(\mathbf{X}, \theta') \leq t | \theta' \in A(\theta), \Gamma) &\geq \mathbb{E}[\widehat{H}_B(t|\theta) | \theta' \in A(\theta), \Gamma] - \varepsilon \\ &\geq \mathbb{E}[H(t|\theta) | \theta' \in A(\theta), \Gamma] - 2\varepsilon. \end{aligned}$$

Since  $H(t|\theta)$  is constant (not random), it follows that

$$\begin{aligned} \mathbb{P}(\tau(\mathbf{X}, \theta') \leq t | \theta' \in A(\theta), \Gamma) &\geq \mathbb{E}[H(t|\theta) | \theta' \in A(\theta), \Gamma] - 2\varepsilon \\ &= H(t|\theta) \mathbb{E}[1 | \theta' \in A(\theta), \Gamma] - 2\varepsilon \\ &= H(t|\theta) - 2\varepsilon. \end{aligned}$$

Thus, for any  $t \in \mathbb{R}$ :

$$\begin{aligned} \mathbb{P}(\tau(\mathbf{X}, \theta') \leq t | \theta' \in A(\theta)) &\geq \mathbb{P}(\tau(\mathbf{X}, \theta') \leq t | \theta' \in A(\theta), \Gamma) \mathbb{P}(\Gamma) \\ &\geq (1 - \delta)(H(t|\theta) - 2\varepsilon) \\ &= H(t|\theta) - \delta H(t|\theta) - 2(1 - \delta)\varepsilon \\ &\geq H(t|\theta) - \delta - 2\varepsilon + 2\delta\varepsilon \\ &\geq H(t|\theta) - \delta - 2\varepsilon. \end{aligned}$$

In a similar manner, we can show that

$$\mathbb{P}(\tau(\mathbf{X}, \theta') \leq t | \theta' \in A(\theta), \Gamma) \leq H(t|\theta) + 2\varepsilon.$$

Following (Meinshausen and Ridgeway, 2006, Assumption 3), we assume there exists  $0 < \gamma < 0.5$  such that  $\mathbb{P}(\theta' \in A(\theta)) \geq \gamma B$ . This assumption is reasonable, as it implies that the partitions (i.e., the leaves) generated by the tree-based estimators are uniformly well-populated. In other words, each leaf contains a sufficient number of observations, ensuring that the coverage properties hold consistently across the partitions. Therefore,

$$\begin{aligned} \mathbb{P}(\tau(\mathbf{X}, \theta') \leq t | \theta' \in A(\theta)) &\leq \mathbb{P}(\tau(\mathbf{X}, \theta') \leq t | \theta' \in A(\theta), \Gamma) \mathbb{P}(\Gamma) + \frac{\delta}{\gamma B} \\ &\leq \mathbb{P}(\tau(\mathbf{X}, \theta') \leq t | \theta' \in A(\theta), \Gamma) + \delta \\ &\leq H(t|\theta) + 2\varepsilon + \delta. \end{aligned}$$

Thus, for any  $\varepsilon, \delta > 0$  and any  $t \in \mathbb{R}$ :

$$|\mathbb{P}(\tau(\mathbf{X}, \theta') \leq t | \theta' \in A(\theta)) - H(t|\theta)| \leq 2\varepsilon + \delta.$$

Taking  $t = \widehat{C}_{\theta, B}(1 - \alpha)$ , by the construction of the empirical quantile over  $A(\theta)$ ,

$$|(1 - \alpha) - H(\widehat{C}_{\theta, B}(1 - \alpha)|\theta)| \leq 2\varepsilon + \delta,$$

which is equivalent to

$$|(1 - \alpha) - \mathbb{P}(\theta \in \widehat{R}_B(\mathbf{X})|\theta)| \leq 2\varepsilon + \delta.$$

Since we can make  $\varepsilon$  and  $\delta$  arbitrarily small by choosing  $B$  large enough, we conclude that

$$\lim_{B \rightarrow \infty} \mathbb{P}(\theta \in \widehat{R}_B(\mathbf{X})|\theta) = 1 - \alpha.$$

■